US006125079A

# United States Patent [19]

Birchak et al.

[11] Patent Number: 6,125,079

[45] Date of Patent: Sep. 26, 2000

[54] **SYSTEM AND METHOD FOR PROVIDING DUAL DISTANCE TRANSDUCERS TO IMAGE BEHIND AN ACOUSTICALLY REFLECTIVE LAYER**

[75] Inventors: **James R. Birchak**, Spring; **Batakrishna Mandal**, Missouri City; **James E. Masino**, Houston; **John W. Minear**, Hudson; **Thomas E. Ritter**, Katy, all of Tex.

[73] Assignee: **Gas Research Institute**, Chicago, Ill.

[21] Appl. No.: **08/856,113**

[22] Filed: **May 14, 1997**

[51] **Int. Cl.**[7] ..... **G01V 1/40**; G01V 1/00

[52] **U.S. Cl.** ..... **367/35**; 367/28; 181/104; 181/106

[58] **Field of Search** ..... 367/28, 35, 69; 340/55; 181/176, 106, 104

[56] **References Cited**

U.S. PATENT DOCUMENTS

| | | | |
|---|---|---|---|
| 3,265,151 | 8/1966 | Anderson | 181/0.5 |
| 3,668,619 | 6/1972 | Dennis | 340/15.5 BH |
| 3,736,552 | 5/1973 | Sessler et al. | 340/5 MP |
| 3,745,812 | 7/1973 | Korpel | 73/67.5 R |
| 3,747,702 | 7/1973 | Beil | 181/0.5 BE |
| 3,978,939 | 9/1976 | Trouiller | 340/55 |
| 4,003,244 | 1/1977 | O'Brien et al. | 73/67.8 R |
| 4,130,816 | 12/1978 | Vogel et al. | 340/15.5 BH |
| 4,197,921 | 4/1980 | Alphonse et al. | 181/176 |
| 4,255,798 | 3/1981 | Havira | 367/35 |
| 4,283,953 | 8/1981 | Plona | 73/589 |
| 4,293,933 | 10/1981 | Park et al. | 367/25 |
| 4,524,433 | 6/1985 | Broding | 367/25 |
| 4,596,143 | 6/1986 | Norel | 73/598 |
| 4,601,024 | 7/1986 | Broding | 367/86 |
| 4,607,352 | 8/1986 | Seeman et al. | 367/35 |
| 4,641,724 | 2/1987 | Chow et al. | 367/28 |
| 4,665,511 | 5/1987 | Rodney et al. | 367/35 |
| 4,685,091 | 8/1987 | Chung et al. . | |
| 4,685,092 | 8/1987 | Dumont | 367/35 |
| 4,703,427 | 10/1987 | Catala et al. | 364/422 |
| 4,709,357 | 11/1987 | Maki, Jr. | 367/35 |
| 4,727,591 | 2/1988 | Manlove | 455/182 |
| 4,733,380 | 3/1988 | Havira | 367/35 |

(List continued on next page.)

FOREIGN PATENT DOCUMENTS

| | | | |
|---|---|---|---|
| 2011437 | 9/1990 | Canada | G01V 1/40 |
| 0549419 A2 | 6/1993 | France | G01V 1/40 |
| 2249629 | 5/1992 | United Kingdom | G01N 29/16 |

*Primary Examiner*—Christine Oda
*Assistant Examiner*—Anthony Jolly
*Attorney, Agent, or Firm*—Pauley Peterson Kinne & Fejer

[57] **ABSTRACT**

A transducer configuration for use in acoustically imaging a target region behind an acoustically reflective layer includes a sonde having a geometrical center and constructed and arranged to support a plurality of transducers. The system includes a first transducer disposed within the sonde at a first distance from the geometrical center for generating a first acoustic pulse and for receiving a first acoustic signal. The acoustic signal comprises a first reflection from the reflective surface, a first set of fluid multiples arising from reflections between the reflective layer and a surface of the first transducer, and a first signal associated with the target area. The system also includes a second transducer disposed within the sonde at a second distance from the geometrical center for generating a second acoustic pulse and for receiving a second acoustic signal. The second acoustic comprises a second reflection from the reflective surface, a second set of fluid multiples arising from reflections between the reflective layer and a surface of the second transducer and a second signal associated with the target area. A mechanism for receiving and processing signals received by the first and second transducers at time intervals which occur between receipt of the first and second sets of fluid multiples, respectively, wherein signal values at time intervals between receipt of fluid multiples provide acoustic waveforms associated with the target region. Each target region, therefore, has a time interval on at least one of the two waveforms which is free of fluid multiples.

**21 Claims, 12 Drawing Sheets**

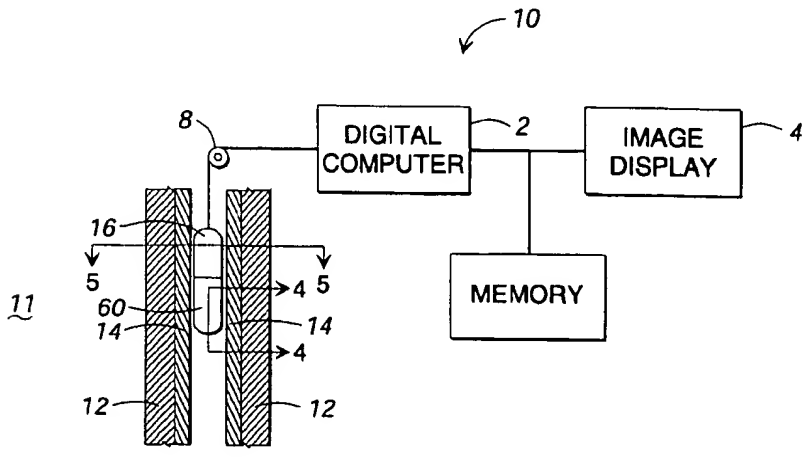

U.S. PATENT DOCUMENTS

| | | | |
|---|---|---|---|
| 4,805,156 | 2/1989 | Attali et al. | 367/35 |
| 4,852,069 | 7/1989 | Clerke et al. | 367/69 |
| 4,867,264 | 9/1989 | Siegfried | 181/105 |
| 4,885,723 | 12/1989 | Havira et al. | 367/35 |
| 4,928,269 | 5/1990 | Kimball et al. | 367/35 |
| 4,999,817 | 3/1991 | Zimmer | 367/65 |
| 5,001,676 | 3/1991 | Broding | 367/31 |
| 5,031,155 | 7/1991 | Hsu | 367/25 |
| 5,081,613 | 1/1992 | Holzhausen et al. | 367/86 |
| 5,097,482 | 3/1992 | Serizawa et al. | 375/12 |
| 5,146,050 | 9/1992 | Strozeski et al. | 181/102 |
| 5,162,994 | 11/1992 | Torres | 364/422 |
| 5,164,548 | 11/1992 | Angehrn | 181/103 |
| 5,184,623 | 2/1993 | Mallart | 128/661.01 |
| 5,212,353 | 5/1993 | Rambow et al. | 181/106 |
| 5,214,614 | 5/1993 | Baule | 367/58 |
| 5,216,638 | 6/1993 | Wright | 367/35 |
| 5,228,006 | 7/1993 | Sheriff | 367/103 |
| 5,228,007 | 7/1993 | Murakami et al. | 367/103 |
| 5,233,993 | 8/1993 | Kawano et al. | 128/660.07 |
| 5,235,857 | 8/1993 | Anderson . | |
| 5,235,983 | 8/1993 | Iida et al. | 128/660.07 |
| 5,235,984 | 8/1993 | D'Sa | 128/660.07 |
| 5,245,586 | 9/1993 | Hassler | 367/12 |
| 5,249,577 | 10/1993 | Shinomura et al. | 128/660.05 |
| 5,251,047 | 10/1993 | Kizu et al. | 358/471 |
| 5,257,265 | 10/1993 | Su et al. | 370/100.1 |
| 5,377,160 | 12/1994 | Tello et al. | 367/35 |
| 5,392,652 | 2/1995 | Levesque et al. | 73/629 |
| 5,418,335 | 5/1995 | Winbow | 181/106 |
| 5,491,668 | 2/1996 | Priest | 367/35 |

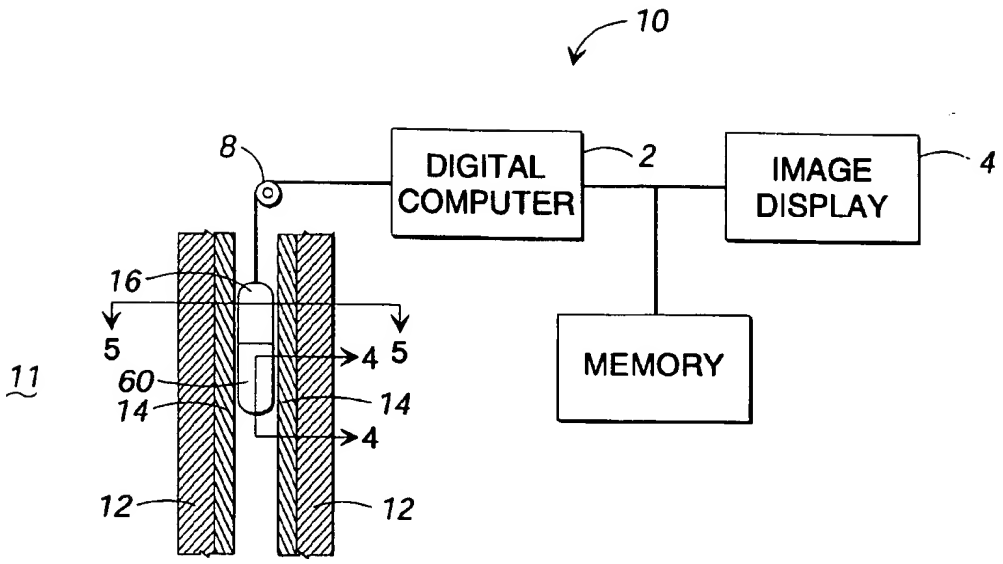
10
8
DIGITAL COMPUTER
2
IMAGE DISPLAY
4
MEMORY
16
5
5
11
60
14
4
5
14
4
12
12

FIG. 1

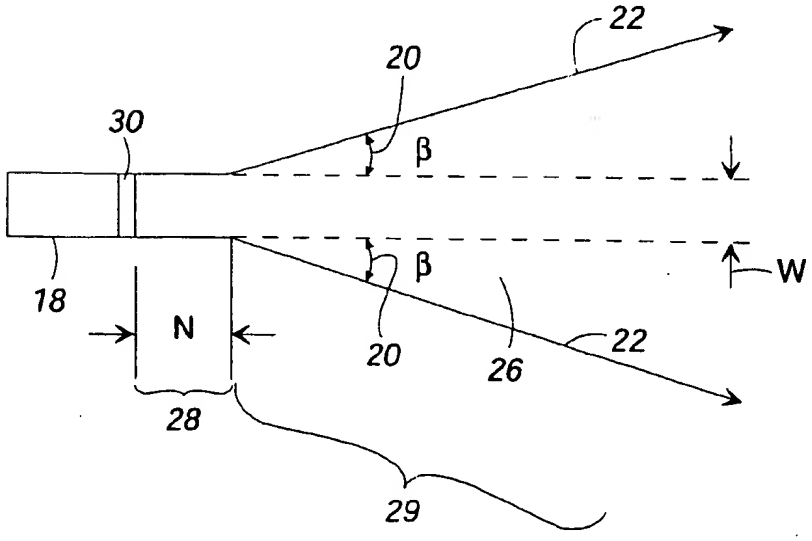
22
20
30
β
β
W
18
N
20
26
22
28
29

FIG. 2

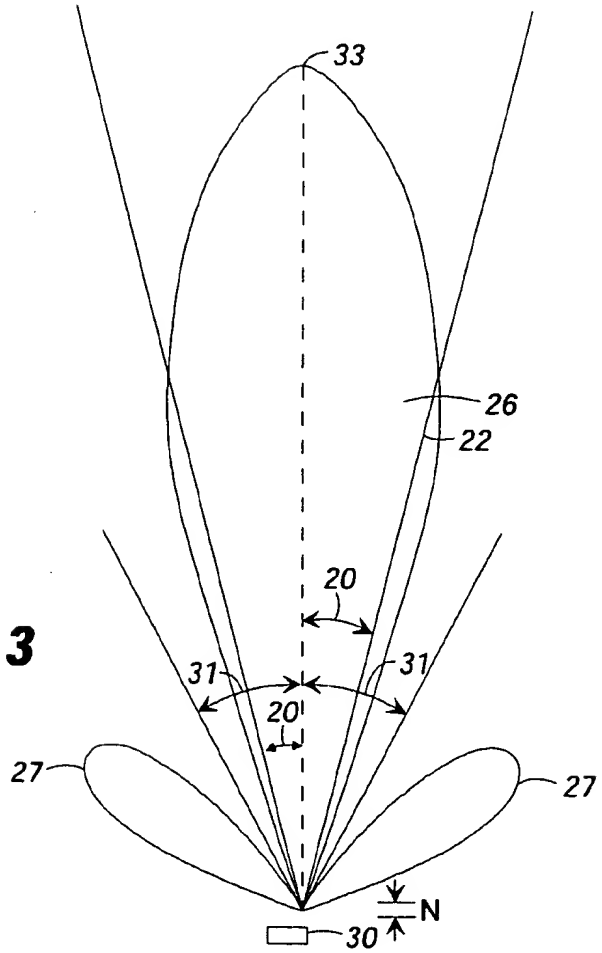
33
26
22
20
31
31
20'
27
27
N
30

FIG. 3

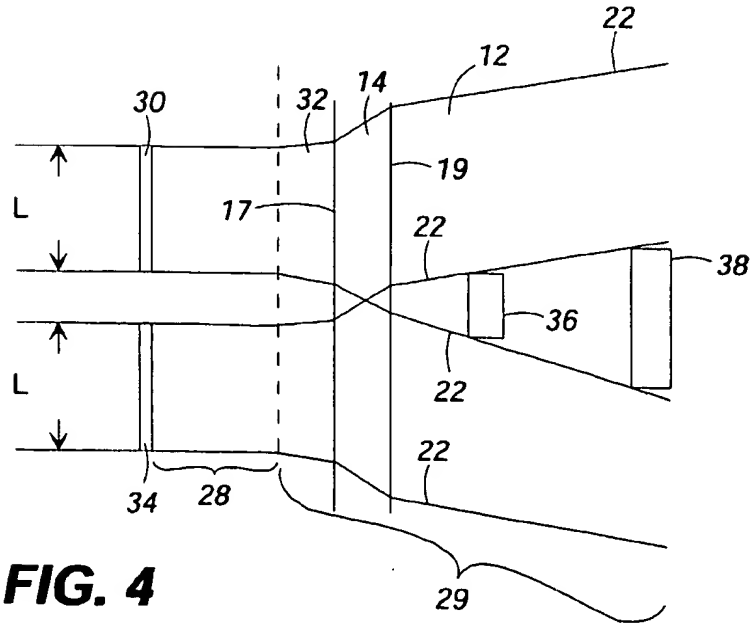
22
12
14
30
32
19
L
17
22
38
36
L
22
22
34
28
29

FIG. 4

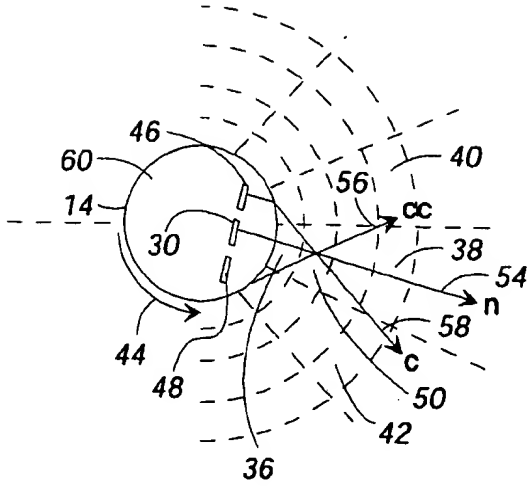


FIG. 5

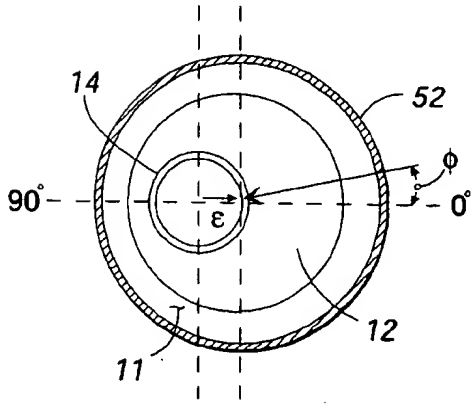


FIG. 6

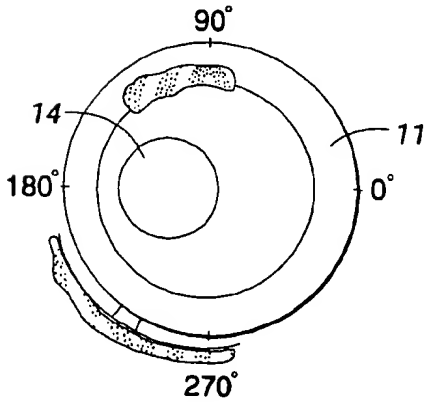


FIG. 7

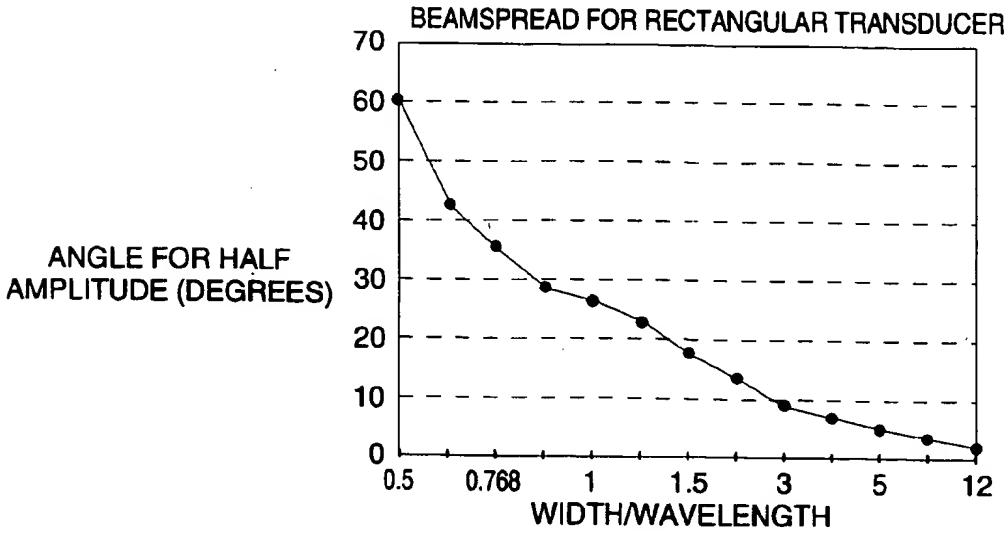
BEAMSPREAD FOR RECTANGULAR TRANSDUCER
ANGLE FOR HALF AMPLITUDE (DEGREES)
70
60
50
40
30
20
10
0
0.5
0.768
1
1.5
3
5
12
WIDTH/WAVELENGTH

FIG. 8

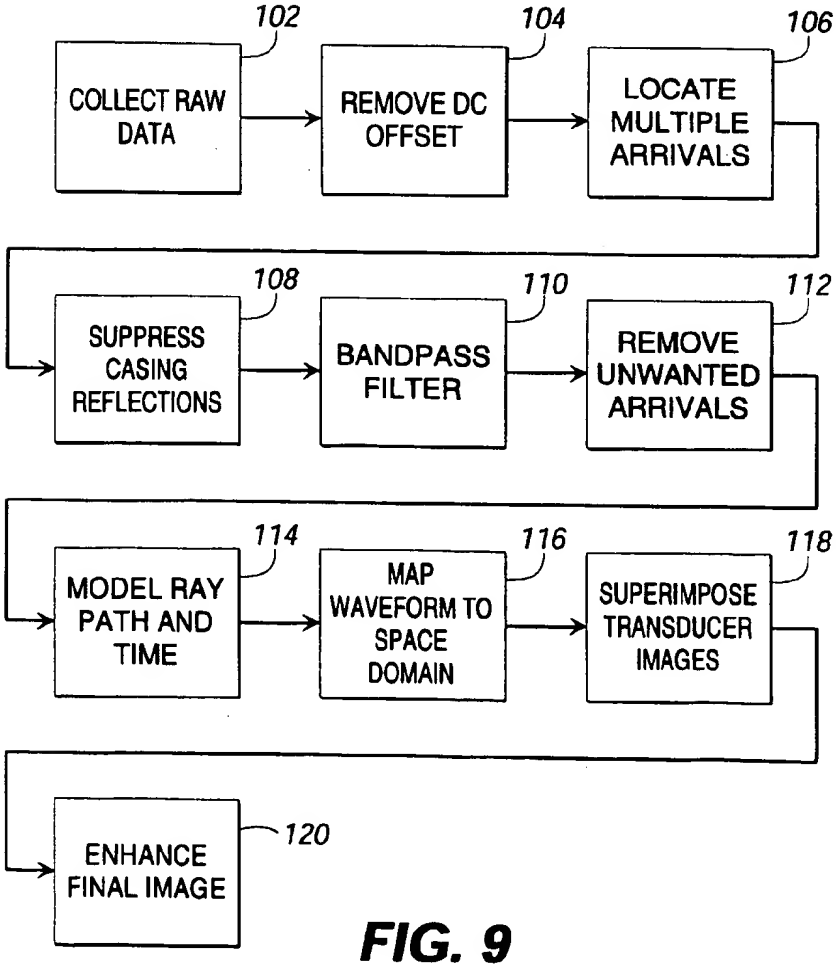
102
COLLECT RAW DATA
104
REMOVE DC OFFSET
106
LOCATE MULTIPLE ARRIVALS
108
SUPPRESS CASING REFLECTIONS
110
BANDPASS FILTER
112
REMOVE UNWANTED ARRIVALS
114
MODEL RAY PATH AND TIME
116
MAP WAVEFORM TO SPACE DOMAIN
118
SUPERIMPOSE TRANSDUCER IMAGES
120
ENHANCE FINAL IMAGE

FIG. 9

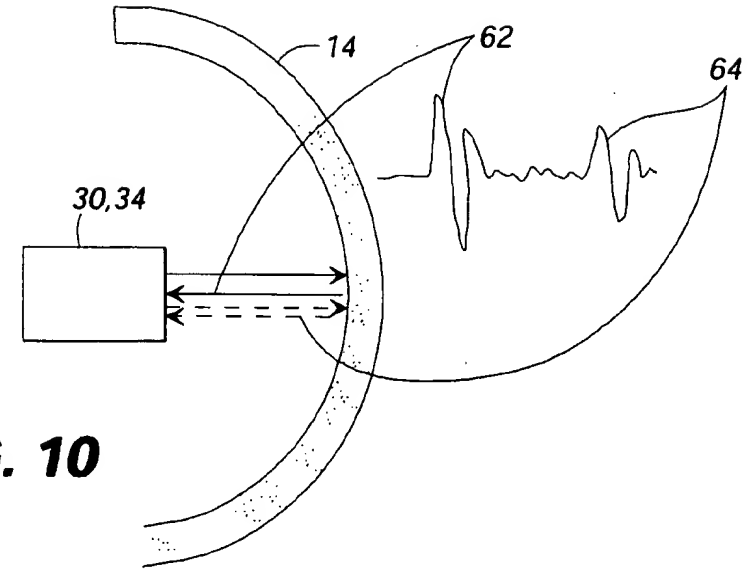


FIG. 10

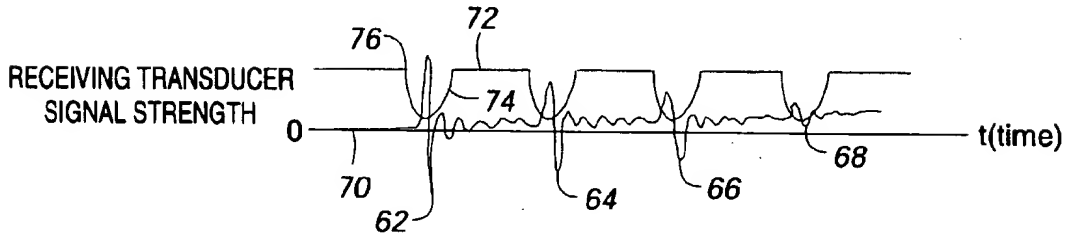


FIG. 11

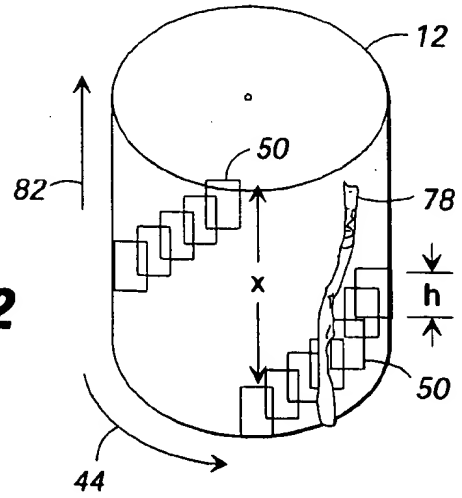


FIG. 12

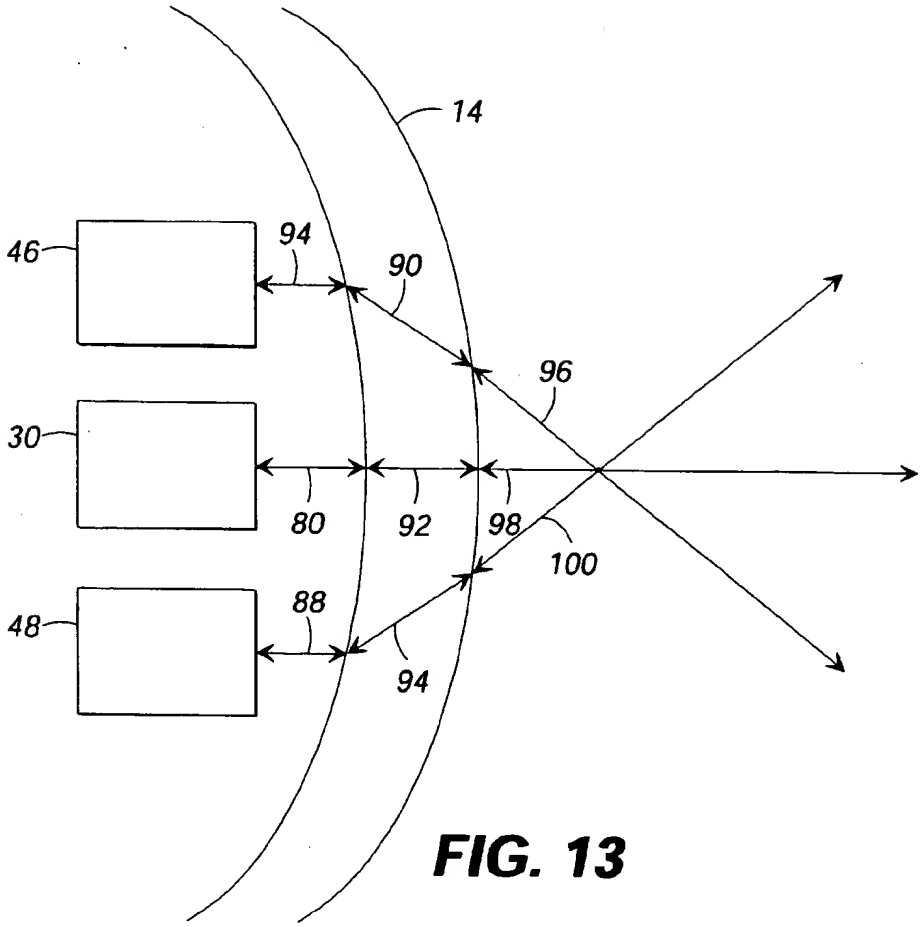


FIG. 13

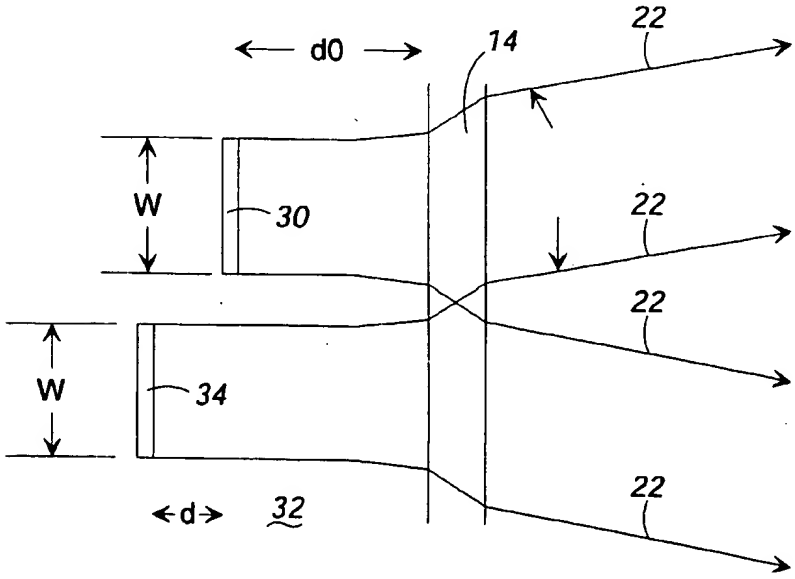


FIG. 14

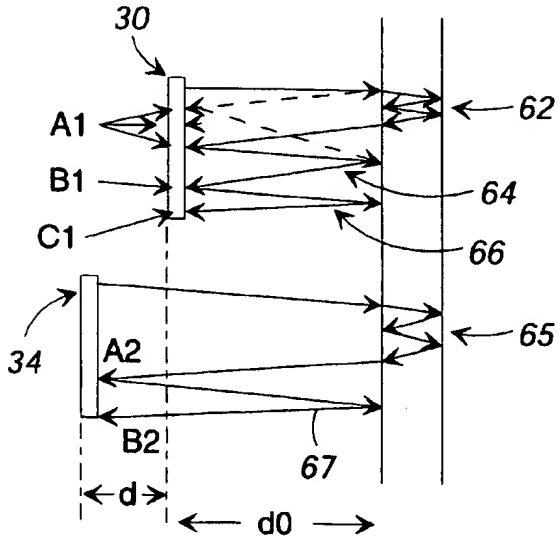
30
A1
B1
C1
62
64
66
34
A2
65
B2
67
d
d0

FIG. 15

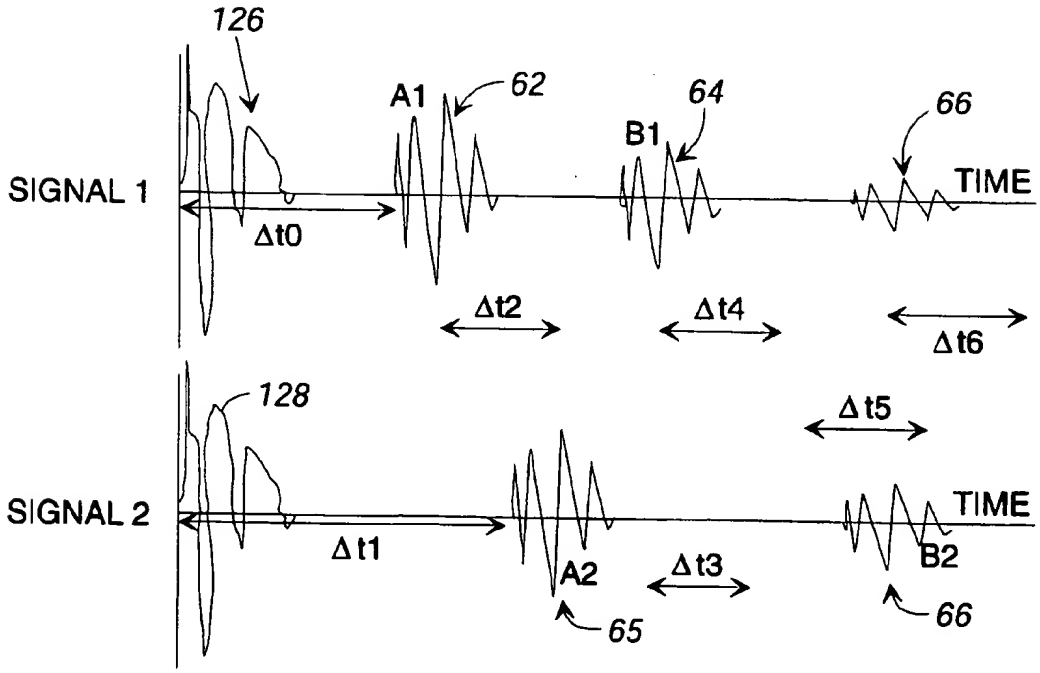
126
A1
62
64
B1
66
SIGNAL 1
TIME
Δt0
Δt2
Δt4
Δt6
128
Δt5
SIGNAL 2
TIME
Δt1
A2
Δt3
B2
65
66

FIG. 16

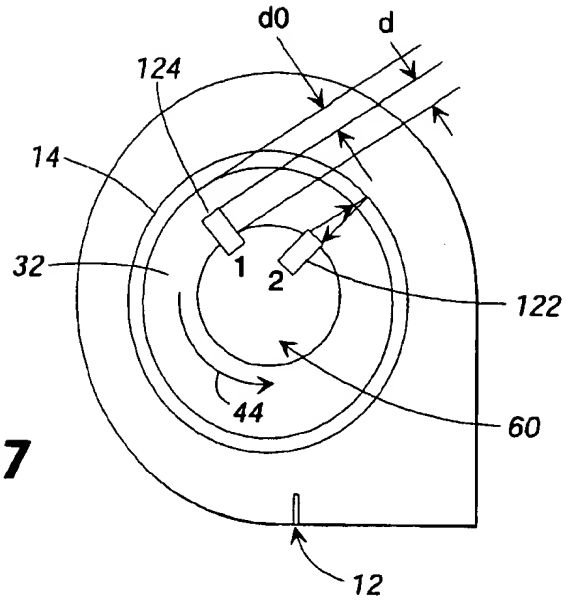


FIG. 17

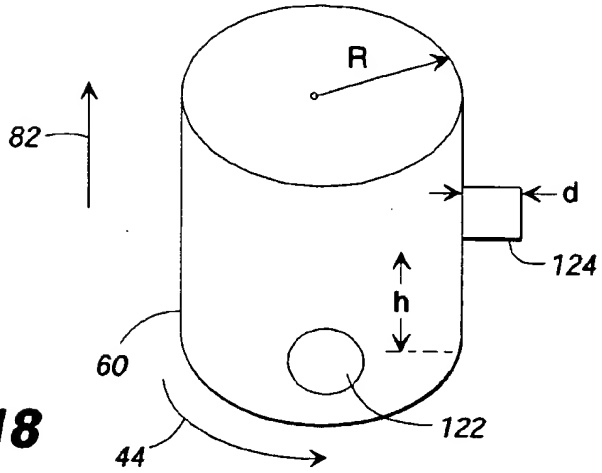


FIG. 18

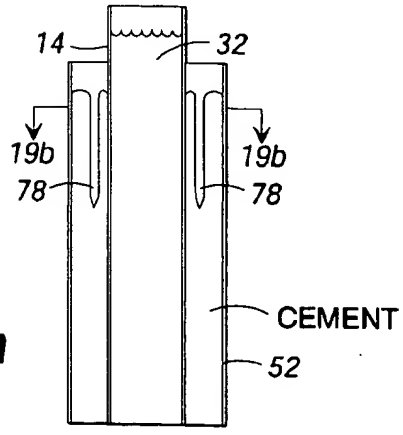


FIG. 19a

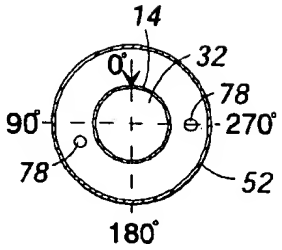


FIG. 19b

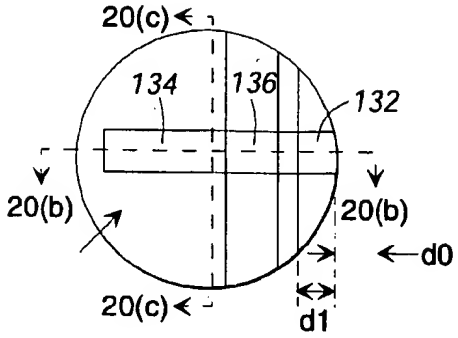


FIG. 20(a)

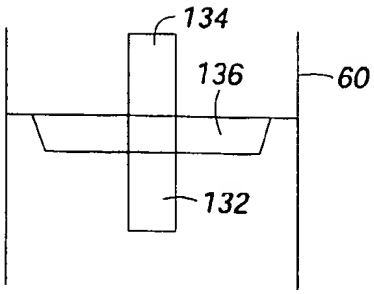


FIG. 20(c)

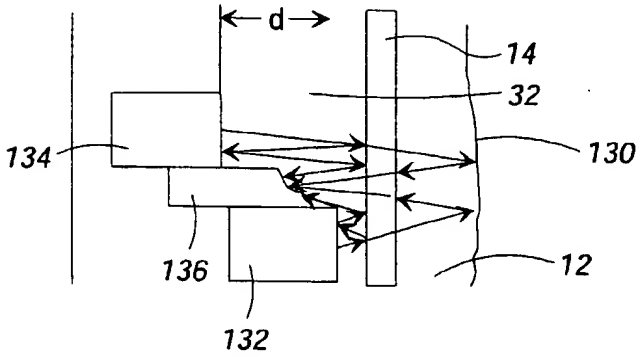


FIG. 20(b)

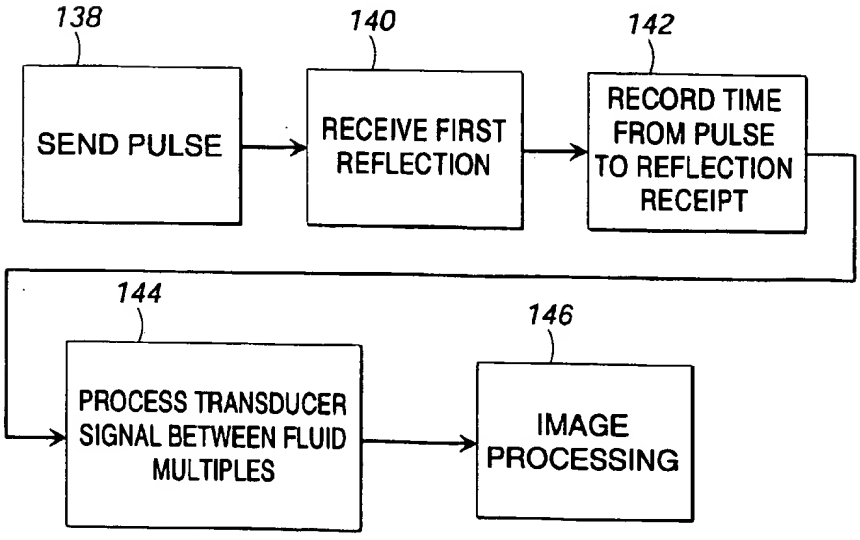


FIG. 21

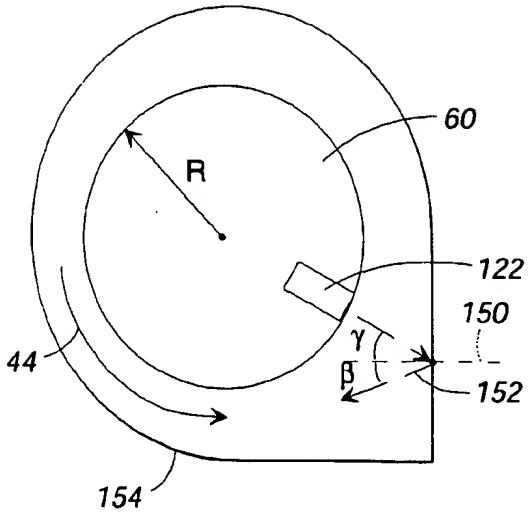


FIG. 22

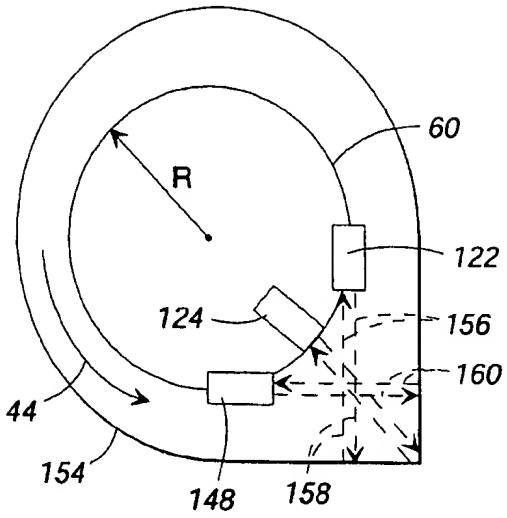


FIG. 23

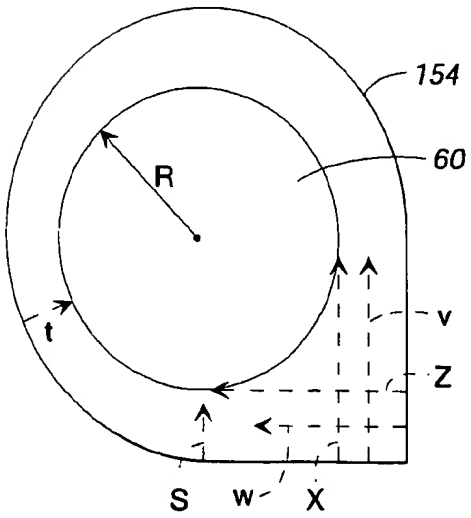


FIG. 24

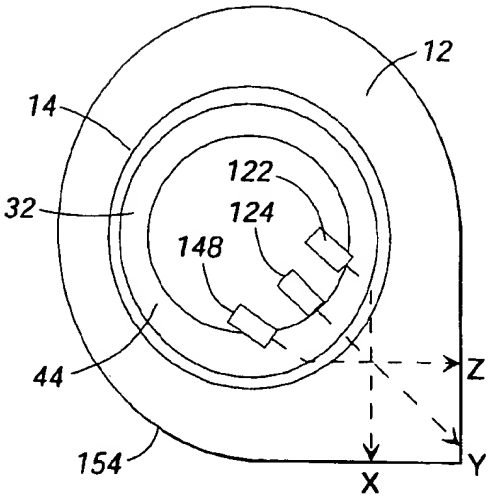


FIG. 25

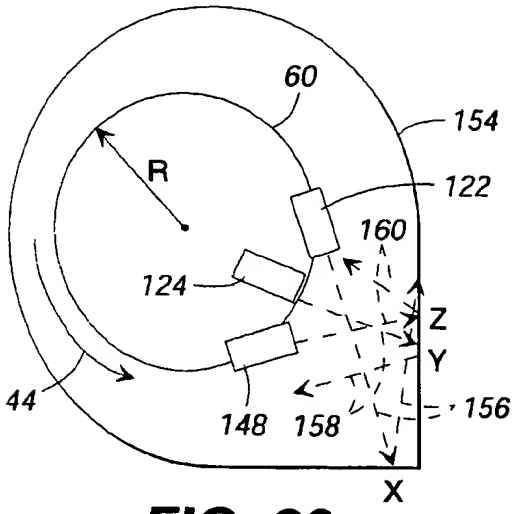


FIG. 26

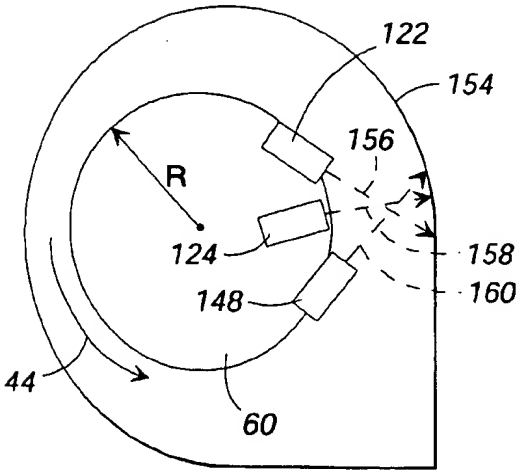


FIG. 27

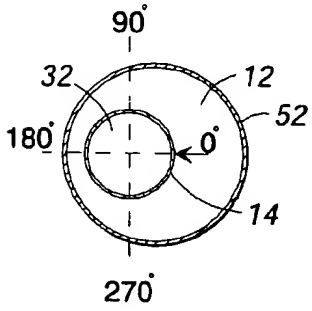


FIG. 28a

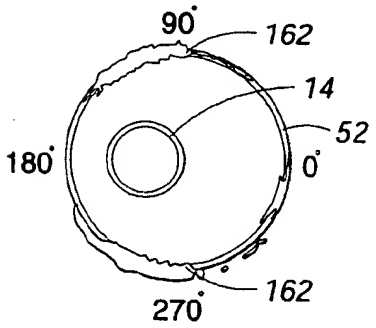


FIG. 28b

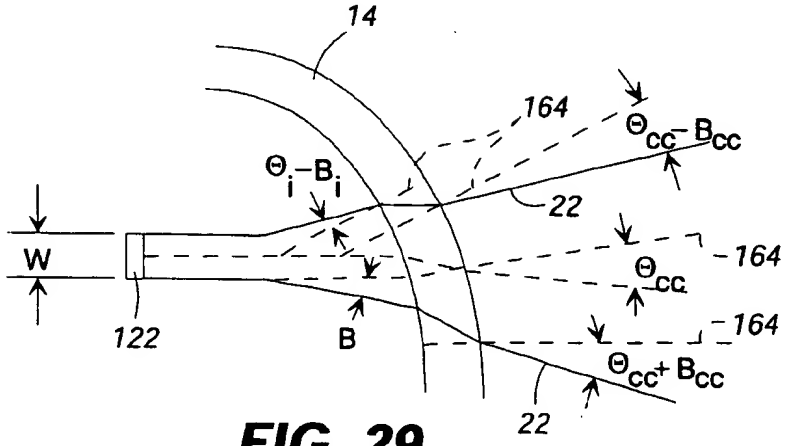


FIG. 29

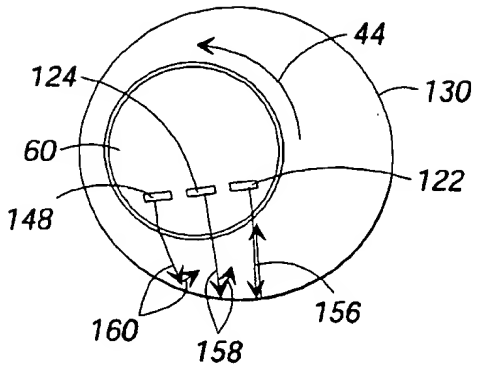


FIG. 30

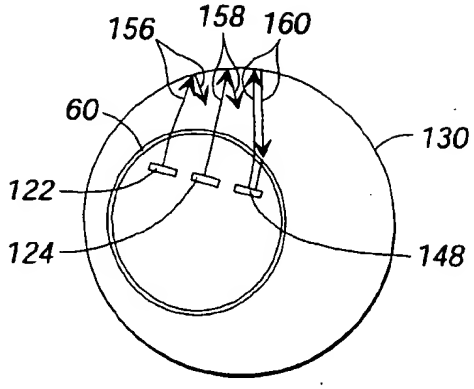


FIG. 31

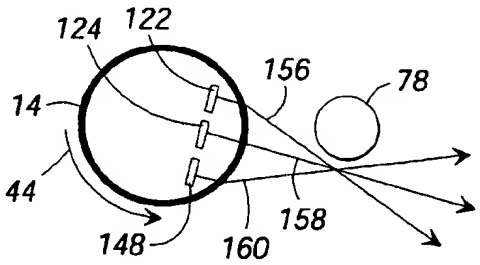


FIG. 32a

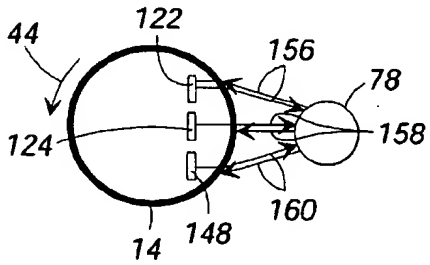


FIG. 32b

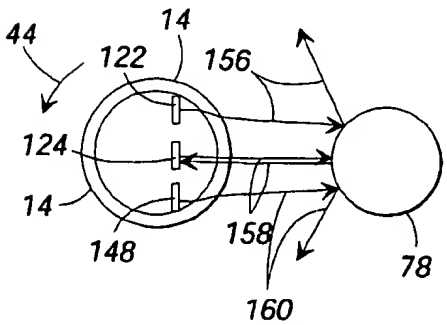


FIG. 33

# SYSTEM AND METHOD FOR PROVIDING DUAL DISTANCE TRANSDUCERS TO IMAGE BEHIND AN ACOUSTICALLY REFLECTIVE LAYER

## RELATED CO-PENDING APPLICATIONS

The following related applications are co-pending: (1) Utility application Ser. No. 08/856,115, filed on May 14, 1997, entitled "Sensor Configuration For Nulling Reverberations To Image Behind Reflective Layers;" (2) Utility application Ser. No. 08/856,114, filed on May 14, 1997, entitled "A System And Method For Processing Acoustic Signals To Image Behind Reflective Layers;" and (3) Utility application Ser. No. 08/856,112, filed on May 14, 1997, entitled "Transducer Configuration Having A Multiple Viewing Position Feature."

## FIELD OF THE INVENTION

The present invention relates to the non-invasive investigation of the integrity of a structural layer disposed between multiple structural layers. More specifically, the present invention relates to a system for imaging portions of a structural layer which are disposed behind an acoustically reflective layer, wherein the acoustically reflective layer has a greater acoustic impedance than the structural layer.

## BACKGROUND OF THE INVENTION

In drilled wells, a steel casing is set within a wellbore formation to maintain the structural integrity of the entire well and to prevent the wellbore walls from collapsing inward. An annular region defined by the space between the steel casing and the wellbore formation is commonly filled with cement to stabilize the steel casing and to prevent fluid communication between vertically stratified geological zones. This cement must be inspected to confirm its structural integrity and to assure a complete sealing of the annulus between the steel casing and wellbore formation.

Imaging tools which are lowered into the open hole utilizing an electric wireline or cable typically construct a graphic representation of acoustic reflection properties and calculate acoustic travel times from the tool exterior to the wellbore wall. The graphic representation approximates a visual image of the wellbore wall.

Steel has a greater acoustic impedance than the impedances of fluids disposed between the imaging tool and the steel casing. Steel also has a greater acoustic impedance than the cement disposed outside the steel casing. As a result, reflective reflections from inner and outer surfaces of the steel casing frustrate attempts to image areas within the cement located an inch or more behind casing. More specifically, multiple acoustic reflections in the wellbore fluid and within the casing occur simultaneously with the arrival of acoustic reflections from the cement onto the acoustic sensors. Furthermore, strong impedance mismatches at the wellbore fluid-steel and steel-cement boundaries greatly decrease energy propagating into the cement and returning from reflectors in cement and back to the acoustic sensors, therefore increasing the difficulty of imaging the concrete. In drilled wells, steel casing is installed to maintain integrity and to prevent walls from caving. The annular region between casing and formation is filled with cement to prevent fluid communication between different geological zones. This cement must be inspected to confirm complete sealing of the annulus between casing and formation.



Steel has large acoustic impedance compared of fluid inside casing and cement outside casing. The resulting reverberation of energy trapped in casing makes it difficult to image reflectors located behind casing. Multiple reverberations in casing fluid and in casing occur simultaneously with the arrival of echoes from certain cement reflectors. Additionally, strong impedance mismatches at steel boundaries cause echoes from reflectors in cement to be much smaller than reverberation noise.

## DESCRIPTION OF THE PRIOR ART

Many attempts have been made to image structures within wellbores, for example, U.S. Pat. No. 4,255,798 to Havira uses a single transducer which acts as transmitter and receiver in a configuration (pulse-echo) which has a complete overlap of transmitter and receiver radiation patterns and therefore strong reverberations, which precludes the processing of weak acoustic signals from reflected from low acoustic impedance materials with respect to high acoustic impedance steel.

U.S. Pat. No. 5,216,638 to Wright describes a technique for identifying casing thickness and cement acoustic impedance from pulse-echo measurements, however the method also generates unacceptably large reverberations from high acoustic impedance.

U.S. Pat. No. 4,999,817 to Zimmer shows a method which utilizes acoustic pulse-echo techniques for describing a circumferential angle of wellbore casing locations which produce large acoustic reverberations resulting from a poor bond at the steel-cement interface between the wellbore casing and cement sealing structure. This method, however, also produces large reverberations, which precludes the sensing of portions of concrete located radially beyond the steel-cement interface.

European Patent Application No. 0 519 419 A2 to Stanke et al. utilizes a sensing system which comprises separate acoustic transmitter and receiver transducers (hereinafter referred to as "pitch-catch"). Stanke et al. aim centers of the pitch-catch radiation patterns at reflectors of interest within the cement. Although that approach attempts to maximize the cement reflector signal, it does not assure that the casing reverberation and casing refracted acoustic waves are minimized. The reflector signal to reverberation noise ratio is therefore not optimized. Furthermore, the imaging method disclosed by Stanke et al. does not take into account the varying travel times through different materials when opening inspection windows with low reverberation noise.

U.S. Pat. Nos. 4,601,024 and 5,001,676 to Broding disclose axial acoustic transducer configurations having intersecting radiation patterns with side-lobe detection for pitch-catch transducers. Those configurations, however, apply to wellbores which do not have steel casings. Therefore, that transducer configuration is specifically adapted to receive a strong acoustic signal from the first reflecting surface and does not attempt to null reflections from highly reflective surface materials for the express purpose of receiving reflected signals from less acoustically reflective material located between layers of reflective materials. Furthermore, Broding uses a variety of transducers, but does not use dual-distance techniques to reduce fluid reverberations.

U.S. Pat. No. 4,805,156 to Attali et al. avoids reverberations in mud between the casing and sensor array by placing transmitting and receiving transducers in pads that contact the casing surface. That approach, however, responds primarily to refracted waves and records attenuation of refracted waves due to energy loss from cement. Information

is not obtained about reflectors within the concrete which are more than an inch behind the casing.

U.S Pat. Nos. 5,184,623 to Mallart; 5,233,993 to Kawano; 5,235,983 to O'Donnell; 5,228,006 to Sheriff; 5,228,007 to Murakami et al.; 5,251,047 to Kizu et al. describe prior art imaging systems which steered, focused sensor array systems. Those conventional arrays have small elements small as compared to the wavelength, which creates an inordinate amount of elements, which requires heavy processing capability by system hardware and therefore slows data processing considerably.

The prior art also demonstrates considerable effort in the evaluation of wellbore casings and surrounding cement. U.S. Pat. No. 5,162,994 to Torres teaches a method for interpreting surface roughness of the wellbore before casing is installed. U.S. Pat. No. 5,031,155 to Hsu describes a method for compressing acoustic signals downhole and reconstructing signals at the surface. U.S. Pat. No. 5,491,668 to Priest describes a method for interpreting the casing thickness. British Patent No. GB 2 249 629 A to Rutledge also describes a method for determining the properties of the cement behind casing. U.S. Pat. No. 5,212,353 to Rambow et al. describes a method for focusing borehole televiewer transducers. Canadian Patent No. 2,011,437 to Huau describes a method for calibrating a bore-hole televiewer transducer. None of the techniques disclosed above addresses imaging behind a highly reflective layer, however.

Other prior art acoustic methods have addressed beam shaping and imaging. For example, U.S. Pat. No. 5,392,652 to K. J. Levesque et al. describes a method for steering ultrasonic beams. U.S. Pat. No. 5,245,586 to Hassler describes a method for reducing reverberations in a sensing transducer. U.S. Pat. No. 5,257,265 to Su et al. also describes a method for reducing reverberation. Finally, U.S. Pat. Nos. 5,235,984 and 5,249,577 to D'Sa and Shinomura et al., respectively, describe methods of forming ultrasonic images. Each of those prior art references, however, utilizes only a single viewing perspective per viewing position, and do not address the problem of obtain information about material disposed behind a highly reflective layer.

In view of the forgoing disadvantages of the above-referenced prior art imaging and calipering devices, a first object of the present invention is to provide an acoustic transducer configuration which calipers and images a first material disposed behind a second material, wherein the second material has a higher acoustic impedance than the first material.

Another objective is to process signals from acoustic transducers to minimize reverberation noise compared to echoes received from reflectors in cement.

Another object of the present invention is to provide individual transducer elements having an exposed area with dimensions that are larger compared than the transducer operating wavelength.

Another object of the present invention is to provide an instrument that utilizes relatively few elements to perform multiple direction and multiple distance inspections.

Another object of the present invention is to provide a system which processes transducer data at significantly faster speed than with steered, focused transducer arrays to image a material behind a highly reflective layer.

## SUMMARY OF THE INVENTION

Generally speaking, the present invention relates to system and method for acoustically imaging a target region designed and acoustically reflective layer, wherein the system includes the transducer configuration for acquiring acoustic image data from a target region disposed behind an acoustically reflective layer. Specifically, the present invention relates to a system and method for processing data received from the target region by receiving transducers which dectect a first arrival of a first acoustic reflection signal which is associated with a first acoustic pulse from at least one transmitting transducer. A system in accordance with the present invention includes a mechanism for suppressing multiple reflected signals originating from the first acoustic pulse, wherein the suppressing mechanism facilitates the acquisition of image data from the target region disposed behind the reflective layer.

To effectively suppress unwanted reverberation signals received from a surface of the reflective material, the suppressing mechanism includes a mechanism for calculating and storing to a computer memory a peak value of the first acoustic reflection signal, a mechanism for establishing a threshold signal based on the first acoustic reflection signal for storing that signal to memory, a searching mechanism for searching the memory and identifying threshold signal values within the first acoustic reflection signal, and a mechanism for canceling the multiple reflected signals, thereby facilitating acquisition of acoustic data originating from the target region. More specifically, the suppressing mechanism utilizes an adaptive multiplier mechanism for detecting reflected signal values above the threshold value to cancel those reflective signal values which are received by the receiving transducer from the first acoustic pulse.

The adaptive multiplier mechanism includes a time measurement mechanism for determining the arrival time between the first pulse and the first reflection, a storage mechanism for storing arrival times to computer memory, a mechanism for creating a canceling signal having amplitude valleys therein, a mechanism for calculating the starting edge of each value as a multiple of arrival time of the first reflection, and a mechanism for adding the canceling signal multiple value at the starting edge of each reflection signal to cancel reverberations which are received subsequent to the first reflection, thereby enhancing acoustic signal strength received from the target area with respect to reverberation signal strength. The system in accordance with the present invention may also utilize a frequency filter coupled to an output of the receiving transducer to enhance the first reflection signals received from the target area and a mechanism for identifying different reflections from separate transmitting transducers.

The present invention also relates to a system for adaptively compressing and transmitting acoustic signal data from a subterranean location within a wellbore along a wireline to an above ground computing means for reassembling the data and for transforming the acoustic data into image data. The data compression mechanism may include but is not limited to a bandpass filter for filtering out undesired reflection frequencies from the reflection signal, a mechanism for performing a Fourier transformation on the reflection signal, a mechanism for transmitting the Fourier transformed signal uphole, and a mechanism for performing an inverse Fourier transformation of the transformed signals to recreate the reflection signal. The data compression mechanism may further comprise a mechanism for converting reflection signal waveforms having a distinct pattern within a data plane into a wavelet transform having a relative small number of coefficients for narrow bandwidth transmission to the above ground computing means, and a mechanism for reconstructing the data plane using an inverse wavelet transform.

The inventive system also comprises a sonde attached via a wireline to a logging truck, wherein the wireline allows the sonde to be lowered into the wellbore. The sonde includes a rotatable sonde head for supporting and housing the transducer configuration when the sonde head rotates the transducer configuration for azimuthally interrogating multiple portions of the target region. The system also includes a means for moving the sonde in an axial direction for axially interrogating multiple portions of the target region, and a control mechanism for adjusting the axial and azimuthal sonde head movement to allow the transducer configuration to acquire overlapping data in the azimuthal and axial directions, wherein overlapping in the azimuthal direction assures occlusion detection within the target region during each complete rotation of the sonde head.

The transducer configuration of the inventive system may comprise at least two transmitting transducers wherein each of the transducers includes a separate radiation pattern. The radiation pattern of each transducer intersects in an intersection voxel within the target region, wherein the intersection voxel is interrogated by all transducers for a given azimuthal position of the sonde head to identify the location and orientation of any reflective boundary which may exist in the intersection voxel. In this regard, the system also includes a mechanism for comparing the reflection signal amplitude received from each of the transmitting transducers floor selecting which voxel contains reflective surfaces. Furthermore, the transducer within the transducer configuration producing the strongest reflection amplitude signal from the voxel identifies the refracted angle, thereby giving an orientation of a normal of the reflecting surface. Once the orientation of the normal to the reflective surface is determined, the orientation of an entire occlusion or channel through the target area may be ascertained after interrogation of adjacent voxels.

The present invention also relates to the method for use within a system which utilizes the transducer configuration for acquiring acoustic image data from a target region disposed behind and acoustically reflective layer, wherein the method processes the acoustically acquired data to image the target region and wherein the reflective layer and target region are divided into voxels circumferentially disposed about a central point for examination. More specially, the method comprises the steps of transmitting a first acoustic pulse, detecting a first arrival of a first acoustic reflective signal associated with the first acoustic pulse, and suppressing multiple reflective signals from the first acoustic pulse to facilitate the acquisition of image data from the target region. Furthermore, the inventive method may also comprise the steps of calculating and storing to memory a peak value of the acoustic reflection signal, establishing a threshold signal of value based on the first acoustic reflection signal value, storing the threshold signal to memory, searching the memory and identifying threshold signal values in the first acoustic signal, and canceling the multiple reflective signals from the first acoustic reflective signal.

The present invention may also include the steps of detecting reflective signal values above the threshold value and canceling those reflective signal values which are received by the receiving transducer from the first acoustic pulse. In the that regard, the inventive method may also include the steps of determining the arrival time between the first pulse and the first reflection, restoring the arrival times to memory, and generating the canceling signal having amplitude valleys therein, calculating the starting edge of each value as a multiple of the arrival time of the first reflection, and adding the canceling signal multiple value at the starting edge of each reflection signal to cancel reverberations which are received subsequent to the first reflective signal thereby enhancing acoustic signal strength received from the target area with respect to reverberation signal strength.

The inventive method may also include the step of frequency filtering the output of a receiving transducer to enhance signals associated with the target area. The inventive method may also comprise the steps of bandpass filtering the reflection signal data for enhancing the first reflection signals and compressing receiving transducer signals for narrow bandwidth transmission to the surface for further image processing.

The present invention may also relate to a dual distance transducer configuration within a sonde having a geometrical center which is constructed and arranged to support a plurality of transducers, wherein a first transducer is disposed within the sonde at a first distance from the geometrical center. The first transducer may be adapted to generate a first acoustic pulse and may receive a first acoustic signal comprising a first reflection from the reflective surface, a first set of fluid multiples arising from reflections between the reflective layer and a surface of the first transducer, and a first signal associated with the target area.

The dual distance transducer configuration may also include a second transducer disposed within the sonde at a second distance from the geometrical center, wherein the second transducer generates a second acoustic pulse and receives a second acoustic signal comprising a second reflection from the reflective surface, a second set of fluid multiples arising from reflections between the reflective layer and a surface of the second transducer, and a second signal associated with the target area.

Furthermore, the dual distance transducer configuration may include a mechanism for receiving and processing signals received by the first and second transducers at time intervals which occur between receipt of the first and second sets of fluid multiples, respectively, wherein signal values at time intervals between receipt of fluid multiples provide acoustic waveforms associated with the target region without reverberation noise associated with the reflective layer, thereby enhancing signals associated with materials behind the reflective layer.

Another embodiment of the dual distance transducer may include a three transducer set. Specifically, the configuration may include a first transmitting transducer disposed within the sonde at a first distance from the geometrical center, wherein the first transducer includes a beamspread radiation pattern comprising a main lobe diverging from the first transducer, a side lobe disposed laterally adjacent to the main lobe, and a null region disposed between the main and side lobes, wherein the first transducer is adapted to generate a first acoustic pulse.

The second transducer comprises transmitting transducer disposed within the sonde at a second distance from the geometrical center, wherein the second transducer includes a beamspread radiation pattern comprising a main lobe diverging from the second transducer, a side lobe disposed laterally adjacent to the main lobe, and a null region disposed between the main and side lobes. The second transducer generates a second acoustic pulse.

The third transducer in the set is a receiving transducer vertically disposed beneath the first transducer and above the second transducer, and includes a receiving surface disposed at a nonparallel orientation with respect to a vertical plane for detecting echoes from the first and second transducers,

wherein the receiving surface includes a receiving beamspread radiation pattern having a main lobe diverging therefrom receiving surface and the receiving beamspread pattern is constructed and arranged to sufficiently detect echoes from the first and second transmitting transducers, and wherein the nonparallel surface dissipates acoustic reflections therefrom, thereby mitigating reflections arising from the reflective layer.

The invention may also include a method for imaging behind a reflective layer comprising the steps of, placing a first transducer within the sonde at a first distance from the geometrical center, generating a first acoustic pulse with the first transducer, and receiving a first acoustic signal with the first transducer, wherein the first signal comprises a first reflection from the reflective surface, a first set of fluid multiples arising from reflections between the reflective layer and a surface of the first transducer, and a first signal associated with the target area.

The method may also include the step of placing a second transducer disposed within the sonde at a second distance from the geometrical center, generating a second acoustic pulse with said second transducer, and receiving a second acoustic signal with second transducer, wherein the signal comprises a second reflection from the reflective surface, a second set of fluid multiples arising from reflections between the reflective layer and a surface of the second transducer, and a second signal associated with the target area.

Finally, the inventive method may include processing signals received by the first and second transducers at time intervals which occur between receipt of the first and second sets of fluid multiples, respectively, wherein signal values at time intervals between receipt of fluid multiples provide acoustic waveforms associated with the target region, free of reverberations associated with the reflective layer.

## BRIEF DESCRIPTION OF THE DRAWINGS

FIG. **1** illustrates a schematic view of a sonde disposed in a cased wellbore for the purpose of imaging and calipering various structural layers within the wellbore.

FIG. **2** illustrates an example of a radiation pattern configuration for a rectangular transducer, wherein the beam is collimated in a near field zone and diverges therefrom.

FIG. **3** illustrates the radiation pattern configuration for the rectangular transducer of FIG. **2**, further illustrating the radiation pattern in the far field.

FIG. **4** is a partial section taken along line **2**—**2** of FIG. **1**, illustrating an example of a radiation pattern configuration for rectangular vertically tandem transmitter and receiver transducers with overlapping main lobes selected to enhance voxels in cement while reducing casing reverberation reception.

FIG. **5** is a partial cross-section taken along line **3**—**3** of FIG. **1**, illustrating a top view of an alternative embodiment for multiple viewing-position imaging transducer configuration, comprising three pairs of transmitting and receiving transducers, wherein each pair is arranged in the vertically tandem configuration, as disclosed in FIG. **4**.

FIG. **6** is a sectional view of a test wellbore configuration including a central casing and a cement annulus surrounding and supporting the casing.

FIG. **7** illustrates an image formed from the information acquired by the transducer configuration of the present invention, wherein darker portions of the image represent stronger reflections from the structural material under examination.

FIG. **8** shows beamspread angle (half-amplitude for pulse-echo) as a function of the aperture parameter, wherein the aperture parameter is expressed as the ratio of transducer width to pulse wavelength.

FIG. **9** illustrates a block diagram of the algorithm of the processing sequence for imaging behind reflective layers in accordance with the present invention.

FIG. **10** illustrates multiples of reverberations subsequent to first a acoustic reflection arrival.

FIG. **11** illustrates a time domain adaptive multiplier signal which suppresses undesired reflection reverberations.

FIG. **12** illustrates an example of a data collection technique in accordance with the present invention wherein consistent voxel configurations overlap in the azimuthal direction but do not overlap in the axial direction.

FIG. **13** illustrates a schematic diagrarm of acoustic ray paths emanating from three transmitting transducers, each leaving different image paths in the image plane.

FIG. **14** illustrates a sectional view an example of a radiation pattern configuration for rectangular, vertically tandem transmitter and receiver transducers positioned at dual distances from the sonde geometric center, with overlapping main lobes selected to enhance voxels in cement while reducing casing reverberation reception.

FIG. **15** illustrates the transducer configuration of FIG. **14**. schematically representing ray tracing of wave propagation for transducers with two different path lengths in fluid.

FIG. **16** illustrates the signals obtained for the dual distance transducers shown in FIG. **15**.

FIG. **17** illustrates an alternative embodiment of the transducer configuration having two transducers embedded in the sonde head at different azimuths in the radial plane.

FIG. **18** schematically illustrates vertical and radial distance between two pulse-echo transducers embedded within a sonde head.

FIG. **19**(*a*) illustrates a sectional side view of a cylindrical test wellbore configuration including a central casing, a cement annulus surrounding and supporting the casing, and several test channels formed in the cement annulus.

FIG. **19**(*b*) illustrates a section view of the cylindrical test wellbore configuration taken along line **19**(*b*)—**19**(*b*) of FIG. **19**(*a*).

FIG. **20**(*a*) illustrates a top view of a sonde head having dual-distance transducers at a single azimuthal location.

FIG. **20**(*b*) illustrates a sectional view of the sonde head of FIG. **20**(*a*) taken along line **20**(*b*)—**20**(*b*).

FIG. **20**(*c*) illustrates a sectional view of the sonde head of FIG. **20**(*a*) taken along line **20**(*c*)—**20**(*c*).

FIG. **21** illustrates a block diagram of the algorithm of the processing sequence for imaging behind reflective layers with a duial-distance transducer configuration in accordance with the present invention.

FIG. **22** illustrates a sonde head having only one pulse-echo transducer and its acoustic wave propagation with respect to an acoustically reflective surface.

FIG. **23** illustrates an alternative embodiment of an acoustic transducer configuration having three transducers orientated to receive pulse-echo signals from perpendicular locations from a corner of a reflective surface.

FIG. **24** illustrates normals to an acoustically reflective surface and various locations on the surface which may be images using the invention transducer configuration.

FIG. **25** illustrates an alternative embodiment of the inventive transducer configuration for imaging a surface

behind an acoustically reflective layer by using refracted acoustic waves.

FIG. **26** illustrates scattering of acoustic wave propagation when no transducers within a configuration are aligned with a reflecting surface, which is useful for imaging tilted surfaces.

FIG. **27** illustrates an alternative embodiment of the transducer configuration.

FIG. **28**(*a*) illustrates another test specimen for use with an alternative embodiment of the transducer configuration.

FIG. **28**(*b*) illustrates acoustically image specimen illustrated in FIG. **28**(*a*), wherein the specimen includes an inner casing eccentered relative to a cement-steel casing boundary.

FIG. **29** illustrates a top view of a beamspread of a rectangular transducer pair which provides the image illustrated in FIG. **28**, having half amplitude paths that refract clockwise at the cement-steel casing boundary.

FIG. **30** illustrates a sonde head orientation for a clockwise angle beam transducer to detect cement-formation reflection for a lower half of an eccentered casing.

FIG. **31** illustrates a sonde head orientation so that a counterclockwise transducer obtains a cement-formation reflection from the eccentered casing.

FIG. **32**(*a*) illustrates a schematic top view of the inventive transducer configuration aimed at a region having no occlusions or channels.

FIG. **32**(*b*) illustrates a schematic top view of the inventive transducer configuration aimed at a region having a channel therethrough, wherein all transducers receive signals when the intersection point coincides with the center of the channel.

FIG. **33** illustrates an alternative embodiment of the transducer configuration shown in FIGS. **32**(*a-b*), wherein the transducer orientation has a beam intersection point outside of the channel.

## DETAILED DESCRIPTION OF THE INVENTION

Referring now to the drawings, FIG. **1** illustrates an acoustic logging apparatus, shown generally as **10**, located in a wellbore **13** in a subterranean formation. Wellbore **13** receives a cylindrical steel casing **14** therein for maintaining structural integrity of the wellbore **13** within the subterranean formation. An annular space between an outer periphery of the casing **14** and an inside surface of the wellbore **13** receives a cement pour **12** for bolstering the structural integrity of the of the wellbore **13** and for sealing various strata of the subterranean formation from one another.

The logging apparatus **10** may include, among other components, a reeling apparatus which winds and unwinds it wireline **8** from a wireline logging vehicle (not shown). Wireline suspends a centralized imaging tool or sonde **16** which may image various structural material layers within the wellbore **13**. Generally, the sonde **16** may include a rotating head **60** at a bottom portion thereof for effectuating a complete circumferential image sweep of the wellbore **13**. More specifically, during a imaging and calipering session, head **60** rotates circumferentially (azimuthally) as the tool moves upward, creating a helical inspection path within the wellbore **13**. In accordance with the present invention, cylindrical tool **16** includes acoustic transducer configuration specifically designed to null reflections from the steel casing **14** and to enhance acoustic reflections received from the cement **12**. Head **60** also includes directional sensors therein for recording an azimuth of the head.

Additionally, logging sensors at the surface or on board the logging vehicle record elevation in the well. Digital computer **2** includes means for receiving and processing acoustic waveform signals received from receiving transducers within the acoustic transducer configuration for the purpose of constructing an image which is representative of the structural integrity of the structural layers of interest. Additionally, digital computer **2** includes means for processing acoustic waveform signals for the purpose of calipering thickness of various structural layers within the wellbore. Apparatus **10** also includes memory **6** for storing all sensing data to memory for further analysis or processing. Finally, the logging apparatus includes an image display **4** for viewing an image constructed by the processing functions of the digital computer **2**.

FIG. **5** illustrates circumferential spatial divisions in terms of circumferential sections or voxels centered on a center line of the cylindrical caisling **14**. Each transducer includes a planar radiation pattern center. Each of those planes intersect. Depending on the focal area of a particular sensor configuration, the rotating head **60** of the sonde **16** will image each voxel to determine the structural integrity of each material disposed in the wellbore. Generally, the transmitting transducer excitement rate and the angular velocity of the head determine the amount of sensing overlap between adjacent voxels. For example, as angular velocity of the head **60** increases, sensing overlap decreases. The voxel demarcations are useful for describing effectiveness of the inventive transducer configuration, as is explained in greater detail below.

I. Transducer Configuration

FIG. **2** illustrates a schenili of an example of a radiation pattern for one dimension (width, w, or length, l) of a rectangular acoustic transducer **30**. As seen in FIG. **2**, an acoustic beamspread pattern radiating from acoustic scensor **30** includes a collimated field zone **28** which has essentially the same width w as transmitting sensor **30** in a near field zone **28**, wherein the near field is defined by a length N. The beamspread pattern diverges beyond near field zone **28** into a transition zone and then into a far field zone. FIG. **2** also illustrates a simplified description of the start of the transition zone **29** by depicting outer peripheries **22** of the start the main lobe **26**. Generally, 50% amplitude contours of the radiation pattern for a transducer in a single medium define the outer peripheries **22** of the far field main lobe **26**. The other dimension, **1**, also has near field, transition and far field zones, but the zone distances depend on length/wavelength. The sensor may include a backing **18** for facilitating propagation of acoustic waves in the desired directions. More specifically, a beamspread angle **20**, illustrates an amplitude contour of the beam in the transition zone **29**. In the true far field of a radiation pattern, a null angle or contour having zero amplitude lies at the contiguous edges of the main lobe and the first side lobe and is greater than angle **20**. Therefore, for purposes of clear illustration, and as further explained below, the null contour falls outside the 50% amplitude contour.

FIG. **3** provides an illustration ot the radiation pattern for transducer **30** in the true far field, wherein the far field is defined by distances from the transducer **30** of greater than 10N, where N is the near field distance, as illustrated in FIG. **2**. As discussed above, the radiation pattern comprises the main lobe **26** having outer peripheries **22** defined by 50% amplitude contours, which diverge from the collimated zone at an angle **20**, defined as the beam spread angle. A center portion of the main lobe **26** is also defined by a 100% amplitude contour **33**. Finally. the radiation pattern may

include sides lobes **27** diverging from the main lobe **26** outside of a null angle **31**. The number of side lobes depends on the ratio of the transducer width/wavelength.

FIG. **4** illustrates a sectional side view in an axial plane of a configuration for transmitting transducer **30** and a receiving transducer **34** which are adapted to image cement **12** behind casing **14**. As is illustrated schematically in FIG. **4**, the present invention configures transmitting and receiving transducers **30** and **34** to create overlapping main lobes selected to enhance acoustic signals received from reflectors in the cement **12** as compared to reverberation signals received from voxels in the casing **14**. As explained above, outer peripheries **22** of the beams represent 50% amplitude contours. In addition to multiple layers of structural materials within the borehole, various fluids **13** within the wellbore may include drilling fluid **32**, as illustrated in FIG. **4** between the transducers **30** and **34** and casing **14**.

FIG. **4** also illustrates near and far voxels **36** and **38**, respectively within the cement **12**. Near voxel **36** includes a smaller area than far voxel **38** because of acoustic beamspread divergence. The present invention utilizes those beamspread patterns to accomplish purposes of the invention. A near surface **17** of the casing **14** nearest the transducers is in a "gap" defined by a non-overlapping zone between the beamspread peripheries **22**. More distant from the sensor configuration, far surface **19** of the casing **14** includes a slight overlapping of the beamspread peripheries. Here it is important to note that this slight overlap creates a much smaller acoustic reverberation reflection attributable to the casing **14** as compared to a large peripheral edge overlap at the casing **14**.

Generally speaking, apertures which house the transmitting and receiving transducers shape the main lobe **26** to create the above-referenced overlapping effect. That approach selects sizes of the transmitter and receiver to produce overlapping radiation patterns in the region behind the reflective layer and non-overlapping radiation patterns in the vicinity of the reflective layer. The present invention is therefore adapted to control the angular widths of the radiation patterns and the steering directions of the centers of the radiation patterns to achieve overlapping in structural layers of interest. The invention includes overlapping of the near field collimated zones behind but not in the reflective layer. The near field configuration, however, requires greater alignment precision than the far field configuration.

For example, with reference to FIG. **4**, transmitting transducer **30** sends energy through a first medium comprising fluid in the borehole disposed between the sonde **16** and the casing **14**. In many cases the first medium may comprise drilling fluid **32**. The transmitted acoustic energy propagates through the first medium and into a second medium having a highly contrasting acoustic impedance with respect to the first medium. In this case, the second medium may comprise steel casing **14**. Thereafter, the transmitted acoustic energy propagates further yet into a third medium, which, in the present case, has an acoustic impedance which is less that that of the second medium. For example, the third medium may comprise cement **12**. Receiving transducer **34** receives echoes from reflectors in the third medium.

Since the second medium has a very high acoustic impedance with respect to the first and third mediums, the second medium (steel casing **14**) causes high energy reverberations which, prior to the present invention, have masked reflections from reflectors in the third medium (cement). However, the transducer configuration of the present invention aims radiation patterns so that second medium echoes occur between collimated transmitter and receiver patterns in the near field. This configuration improves the ratio of third medium reflector signal to reverberation noise.

FIG. **5** schematically illustrates an alternative embodiment of the present invention which utilizes three pairs of transmitting and receiving transducers. In this embodiment, the sonde head **60** rotates in a counterclockwise direction, shown by arrow **44**, as the wireline **8** moves the sonde **16** in a vertical direction within the casing **14** to accomplish complete imaging of the well system. FIG. **5** also illustrates in dashed lines a number of voxels surrounding the sonde **16** which lie within drilling fluid **32**, casing **14** and cement **12** for the purpose of defining the location of intersecting beamspread patterns from various transducer pairs. More specifically, sonde **16** includes counterclockwise angle beam transmitting transducer **48** and a corresponding receiving transmitter disposed axially thereunder (not shown), transmitting transducer **30** and a corresponding receiving transmitter disposed axially thereunder (not shown) and clockwise angle beam transmitting transducer **46** and a corresponding receiving transmitter disposed axially thereunder (not shown).

Each of transmitting transducers **48**, **30** and **46** fire in sequence, beginning with transducer **48** and ending with transducer **46**. As seen from FIG. **5**, transducer **48** transmits counterclockwise beam **56** in a direction of counterclockwise far voxel **40**, transducer **30** transmits normal beam **54** in a direction of normal far voxel **38**, and transducer **46** transmits clockwise beam **58** in a direction of clockwise far voxel **42**. Each of beams **54**, **56**, and **58** intersect within the intersection voxel **50**. If a reflector surface exists in intersection voxel **50**, the beam having the largest reflection will have an orientation closest to being perpendicular to the reflector surface. The radial distance to the intersection voxel **50** is unchanged as the beam direction rotates. Voxels at other radial distances are also interrogated by all three pairs but at different azimuthal orientations of the rotating head. Waveforms are stored in memory and compared to select the orientation of reflector surfaces in each voxel. Additionally, angular velocity of the sonde head **60** controls the number of firings per voxel. Obviously, firings per voxel increases with decreasing angular velocity. As the number of firings per voxel increases, the clarity of any image constructed from received acoustic energy increases. An image is formed by mapping most probable reflector surface orientations for voxels having strong reflector signals. The mapping requires storing data to select surface orientations for voxels at smaller or larger radial distances than the radial distance of the intersection voxel.

FIG. **6** illustrates laboratory test borehole simulation for validating the engineering design of the inventive transducer configuration. The laboratory version of the system places transducers in specimens containing the essential features encountered downhole. More specifically, FIG. **6** illustrates a top, sectional view of a model specimen which includes casing **14** having a fluid (water) disposed therein. The model also includes a cement annulus **12**, an artificial earth formation **11** comprised of sand and epoxy and an outer casing jacket **52**. Cement annulus **12** is comprised of a Class H cement cured at 200 psi pressure. The 0° arrow shows the circumferential location of a casing where scanning begins for the imaging process.

FIG. **7** illustrates an image of specimen having casing eccentered relative to the cement to formation wall. The specimen shown in FIG. **6** was inspected by placing three pairs of transducers within casing **14**, wherein the transducers are arranged into the configuration embodiment illustrated schematically in FIG. **5**. The boundary of formation-

to-outer steel casing is also shown. Darker images show stronger reflections. The gray-scale image coinciding with the circle showing the location of the cement-to-formation boundary shows that the method can detect a weakly reflecting surface.

FIG. **8** shows beamspread angle (half-amplitude for pulse-echo) as a function of the dimensionless aperture parameter, which is a transducer width to acoustic energy wavelength ratio (Width/Wavelength). For the purposes of the present invention, the width may be the narrow or long dimension of the rectangle.

Theoretically speaking, reflectivities and transmissions for normal incidence through a boundary are derived from the acoustic impedance, Z, given by equation (1)

$$Z_i = \rho_i V_i \tag{1}$$

where $\rho_i$ is the density and $V_i$ is the speed of sound for medium i. The reflected amplitude from the boundary is

$$R = \frac{(Z_2 - Z_1)}{(Z_1 + Z_2)} \tag{2}$$

The transmitted amplitude (T) is

$$T = \frac{(2 * Z_2)}{(Z_1 + Z_2)} \tag{3}$$

Conservation of momentum gives

$$T = R + 1 \tag{4}$$

Although equations 1 to 4 over-simplify wave propagation from medium to medium, computer acoustics models may use mathematical relations that account for effects of surface curvature, refraction, attenuation and multimode propagation. With regard to the test specimen illustrated in FIG. **6**, the acoustic impedance $Z_i$ of cement is 6.0 MRayls and the $Z_2$ of the simulated earth formation is 4.4 MRayls, which yields a reflected amplitude R of approximately 0.2. With regard to the above-referenced test specimen, experimentally observed reflected amplitudes R matched the calculated values, thus validating the engineering design.

With the inventive acoustic sensor configuration described herein, weak acoustic reflections attributable to the cement **12** are expressed as the images illustrated in FIG. **7**. Without the inventive sensor array, reflections from the cement-formation boundary were comparable to the reverberation noise and could not be imaged.

FIG. **8** shows beamspread angle expressed in terms of half-amplitude for a pulse-echo sensor configuration, as function of the aperture parameter, which is the ratio of the transducer width, W, to the acoustic energy wavelength. Width, W, may be the narrow or long dimension of the rectangle. The wavelength, $\lambda$, is obtained from

$$\lambda = \frac{V_i}{f} \tag{5}$$

With regard to equation 5, the speed of sound, $V_i$, refers to propagation velocity for acoustic mode i. Frequency $f$, refers to the center of the frequency bandpass. Beamspread angle, $\beta$, shown in FIG. **2**, depends on the definition of half amplitude. Received signals from pulse-echo (or other two-way propagation methods having equivalent transmitter and receiver), have half amplitude angle given in FIG. **8**. A different definition may apply to one-way propagation. At angle, $\beta$, the magnitude of the signal, A, (for one-way propagation) is

$$A = \frac{\mathrm{Sin}(u)}{u} \tag{6}$$

The nondimensional parameter, u, is expressed as

$$u = \frac{\pi w}{\lambda} \sin(\beta) \tag{7}$$

Equation 6 applies to the beamspread of rectangular transducers with the width w as shown in FIG. **2**. For two way propagation (i.e., pulse-echo), the received signal from a reflector at angle, $\beta$, is reduced by the magnitude A for transmission and again by A for reception. The two-way reduction at $\beta$ compared to the straight-ahead ray is therefore $A^2$. As discussed above, FIG. **8** applies to half-amplitude pulse-echo signals, i.e., to $A^2$=0.5. For pulse-echo signals, Equations 6 and 7 are solved using $A=(0.5)^{(05)}$. The near-field distance, N, which is illustrated in FIG. **2** is approximated by

$$N = \frac{w^2}{4 * \lambda} \tag{8}$$

The aperture designs using Equations 5 to 8 include other orientations of the transducer faces than the vertical orientations shown in FIG. **4**. For example, tilting the faces of the transducers in FIG. **4** changes the location of the overlap zone of the transducers. In the experiments to create the image illustrated in FIG. **7**, the transducer faces were tilted approximately 4° toward each other in the axial plane. This tilt angle is needed when the gap between the transmitter and receiver becomes large and reduces the overlap at the near voxel.

In a preferred embodiment of the inventive acoustic sensor configuration, and where imaging typical casings having typical sizes in the field, the configuration uses transducers of similar frequency of approximately 400 kHz. Additionally, the preferred embodiment utilizes transducers having a bandwidth of approximately 400 kHz and a size of approximately 1.0 inch by 0.4 inches. Those parameters are comparable to transducers used in pulse-echo cement bond tools. Such transducers are built to withstand downhole temperatures of at least 350° F. and pressures of up to 20,000 pounds per square inch (psi). Normally, the transducers are mounted on a rotating head similar to that of a conventional pulse-echo tool. The head requires accurate mounting angles and centralization in the bore of the casing to assure that the radiation patterns propagate in the required directions with the required standoff from casing.

The tool for the new technique will require sufficient slip-ring connections from each transducer element to the electronics in the stationary part of the tool. The system may also utilize downhole processing, such as data compression, or a sufficient telemetry data rate to transmit information to the surface which is representative of images of the cement behind casing. The transducer azimuth and elevation in the wellbore must be measured to create images as a function of depth in the well.

As discussed above, the invention also relates to a method for selecting transducer apertures to obtain radiation patterns that overlap in the zone of interest but not in the reflective layer which causes reverberation. Aperture modeling in

accordance with the present invention traces borders on collimated and divergent edges of transducer radiation patterns. The inventive method offers simplified analysis for sizing transducer faces to select beam shape and angle. The aperture model estimates collimation and divergence of beams passing from transmitter through borehole fluid, casing and cement and returning to the receiver.

## II. Image Data Processing

The present invention also provides a unique system and method which improves data processing from the receiving transducers **34** to form images of cement behind casing as illustrated schematically in FIGS. **1** and **9**. More specifically, a data processing procedure in accordance with the present invention may utilize a digital computer **2** in combination with unique sonde hardware to process receiving transducer data downhole, compress transducer data for uphole telemetry over wireline **8**, reconstruct transducer data image transducer data over display **4**, and store image data to memory **6**.

The present invention also optimizes downhole data processing for telemetry on existing wireline systems that transfer information from the wellbore **13** to hardware on the surface. The downhole processing performs transformations that extract useful information from waveforms and reject unwanted reverberations attributable to the casing fluid (e.g., drilling fluid **32**) and the casing wall (e.g. steel casing **14**). A data interpretation algorithm in accordance with the present invention utilizes unique processing methods for selecting the most reflective surface locations and orientations in the media (e.g., cement **12**) behind the reflective layer (e.g. steel casing **14**).

The approach uses processing algorithms on data from multiple transducers to image behind reflective layers, which requires several steps to create images from data produced by receiving transducers **34**, since signals from reflectors behind a strongly reflective layer are difficult to detect. More specifically, impedance mismatches at layer boundaries give weak reflector signals as compared to reverberations, because reverberations occur between the transducer and the first reflector (casing **14**). FIG. **9** illustrates a flowchart of the algorithm of the processing sequence for imaging behind reflective layers in accordance with the present invention. As discussed in greater detail below, receiving transducers **34** collect raw data from azimuthal observations, as indicated by module **102**. The inventive system then removes any DC offset from the received signals as indicated in module **104**. The system then locates multiple arrivals in the data signal, as indicated in module **106**, and suppresses multiple arrivals stemming from casing reflections, as indicated in module **108**. The system then subjects the processed signal to a bandpass filter for further noise reduction, and removes all unwanted arrivals, as indicated in modules **110** and **112**, respectively. The system then models acoustic ray paths with respect to time for receiving transducer, as indicated in module **114**. The system then transforms the time domain waveform amplitude to the space domain based on ray path calculations, as indicated in module **116**. The system then superimposes images created from each of the receiving transducers and enhances the final image, as indicated in modules **118** and **120**, respectively.

As discussed above, the invention includes a method for processing data to obtain images of reflectors behind a highly reflective layer which causes reverberation. The processing includes four features needed for creating images successfully with conventional wireline surface trucks and telemetry: A) enhancement of downhole signals behind the reflective layer: B) adaptive downhole data compression for telemetry; C) calculation of probable reflective surface location and orientation behind the reflective layer; and D) techniques for forming images from the data transmitted to the surface.

### A. Enhancing Signals From Behind Reflective Layers

Detecting signals behind the reflective casing layer requires the discrimination between signals reverberating from the steel casing **14** and reflections associated with the less reflective structural layers behind the casing **14**. In this context, first arrival detection is critical to imaging reflective surfaces behind the casing **14**, because it facilitates the removal of unwanted reverberations from the ray path signal.

#### 1. First and Multiple Arrival Detection

FIG. **10** illustrates multiples of reverberations subsequent to first a acoustic reflection arrival. The transmitting and receiving transducers **30** and **34** are illustrated schematically within casing **14** for the purposes of a functional discussion of the inventive system. Reference numeral **62** indicates the first pulse and reflection of an acoustic signal sent by transmitting transducer **30**, and also indicates the first reflection signal strength as a function of time. In the signal strength versus time plot, the first reflection signal includes a peak amplitude for a given transmitting transducer pulse, which is also indicated by the numeral **62**. Numeral **64** illustrates the second reflected signal as shown in dashed lines as a reverberation of the first pulse from the transmitting transducer surface, to an inside surface of the casing **14**, and back to receiving transducer **34**. The second reflection occurs because of trapped reverberations in the fluid inside the casing. As expected, the peak of the second reflection is less than that of the first reflection, which is due to acoustic energy dissipation associated with the surrounding materials and fluids.

The inventive system calculates the first arrival time by using the peak of the envelope of the signal and a searching mechanism to identify threshold values. As discussed in greater detail below, the inventive system utilizes the first arrival time of the peak of the envelope to effectively suppress unwanted reflection signals. The ring-down time of the first arrival depends on transducer reverberations and casing reverberations. As illustrated in FIG. **10**, after first arrival detection, other multiples are identified. The arrival times of the later arrivals are integer multiple of the first arrival time.

#### 2. Suppressing the Multiples

FIG. **11** illustrates a time domain adaptive multiplier signal which, when multiplied by the processed output of receiving transducers **34**, suppresses undesired reflection reverberations. FIG. **11** also illustrates the acoustic reflection signal strength as a function of time, in a manner which is similar to that of FIG. **10**, but in illustrated greater detail. As seen from the reflection signal, numerals **62**, **64**, **66** and **68** each represent first , second, third and fourth reflections, respectively, from a single pulse originating from transmitting transducer **30**. As discussed above, casing **14** produces the primary and multiple reflected signals **62** through **68**, which are considered to be noise.

The inventive system utilizes several techniques suppressing those signals: 1) Detection of casing reflections using techniques described above; and 2) suppression of those reverberations via the use of a suppressing signal **72** based on first reflection arrival time and peak signal strength illustrated by numeral **62**. FIG. **11** illustrates suppression of

these reverberations with an adaptive multiplier based on the detection algorithm. The valley **74** in the multiplier has a width which is selected from the reverberation time observed for the first reflection. This width depends strongly on reverberation time for the particular casing. The location of the starting edge **76** of each valley in time is calculated as a multiple of the first arrival time of the first reflection. Thus, the system may multiply suppressing signal **72** and reflection signal **70** to eliminate reflection signals **62, 64, 66** and **68**, thereby reducing noise associated with the reflective layer (casing **14**) and facilitating the detection of signals associated with occlusions in layers of material (e.g., cement **12**) behind the reflective layer (casing **14**).

3. Frequency filtering

As discussed above, acoustic impedance mismatches of casing fluid, casing and the material behind the greatly reduce energy transmitted behind the reflective layer represented by the casing. For example, the casing **14**, which has a high acoustic impedance, borders cement **12**. Thus, much of the acoustic signal generated by transmitting transducers **30** is reflected at casing boundaries. In accordance with the present invention, the desired effect is to have receiving transducers **34** receive broadband signals, since the broadband signals include pertinent information about reflectors (e.g. occlusions or unwanted channels in cement **12**) behind casing concentrated in a narrow bandwidth determined by the thickness resonance of the casing. The inventive system then extracts the narrow bandwidth information from the received broadband signal utilizing a bandpass filter. Processing observed waveforms with a bandpass filter enhances reflector signal to reverberation noise. Useable frequencies are typically approximately equal to the thickness resonance frequency of the casing wall. Thickness resonance of such frequencies are typically 250 kHz to 600 kHz.

4. Identifying Different Arrivals

Proper identification of different arrivals (compression, shear, and multiples) is a key factor in creating images. Without proper identification, different arrivals may cause incorrect image reconstruction for the region behind the casing. A single transducer response does not uniquely define different arrivals. Therefore, the inventive system utilizes multiple transducer responses to identify arrivals for valid imaging behind casing.

5. Cross-Referencing the Different Transducers

The multiple viewing position technique has each transducer pair response identify different aspects of wave propagation behind casing. For example, FIG. **5** illustrates a top view of three pairs of transmitting and receiving transducers. The center transducer pair produces large casing reverberations while the off-centered transducer pairs have smaller casing reverberations due to large refracted angles in the casing. These features are used to identify different objects by cross referencing the different transducer responses, as explained in greater detail below.

B. Adaptive Data Transmission

Imaging behind casing requires transmitting large amounts of data uphole. Present telemetry systems have inadequate bandwidth to transmit full waveform data at commercial logging speeds. After signal enhancement by bandpass filtering, the inventive system employs adaptive downhole data compression techniques based on signal characteristics. One of the following three approaches is selected based on waveform characteristics for a particular borehole.

1. Simplified Time Window Summation

Here, each waveform is divided into small number of time windows for independent summing within each time window. Time window lengths depend on voxel size in the space domain and the speed of propagation of acoustic energy through the medium behind casing. Each time window data point represents the contribution of signals from the corresponding voxel. Image resolution in the propagation direction depends on the time window duration. Image resolution in the azimuthal direction depends on the width of the transducer radiation pattern, the distance behind casing and the sampling rate (see FIG. **5**).

2. Dominant Frequencies

To send waveforms to the surface, the system may employ techniques to reject unnecessary frequency information. Such rejection is possible because information about reflectors behind the reflective layer (e.g., casing **14**) exists within a narrow frequency band. As discussed in greater detail below, the system may perform a Fourier Transform on the broadband signal and select only those signals contained within the narrow band of interest. Because only a band of the Fourier components is sent, the system effectively compresses the waveform. The system then reconstructs a close replica of the waveform by zero padding Fourier components and performing an inverse Fourier transform.

3. Wavelet Transform of Full Scan Waveforms as a Pattern

The inventive system employs other means of compressing the signal of interest for uphole telemetry, by utilizing waveform characteristics associated with adjacent voxels in the wellbore. Typically, adjacent voxels in an azimuthal direction of the wellbore **13** will have similar waveforms. This similarity can be used to perform wavelet data compression techniques. For example, coefficients of a wavelet transform represent key contributions to the signal. For band limited signals, only a few wavelet coefficients are needed to reconstruct the waveform above ground, after uphole telemetry. Therefore, selecting only a small number of wavelet coefficients for uphole telemetry effectively compresses the signal for uphole processing. As explained above, imaging behind casing requires multiple observations at different azimuths. Those observations form a data plane having orthogonal coordinates of time and azimuthal position. The waveforms comprising this data plane have a distinctive pattern which the inventive system converts using a wavelet transform having a relatively small number of coefficients. After uphole telemetry, the inventive system then reconstructs the data plane using an inverse wavelet transform.

C. Adaptive Voxel Configurations

The collection of data downhole must give the desired coverage of the volume region behind casing for the system to construct a useful image. For some applications, overlapping in the azimuthal and axial direction is desired. Frequently, imaging systems must utilize overlapping voxels in the azimuthal direction to assure the detection of occlusions or channels which form from the migration of gas vertically through freshly poured cement in a direction opposite to that of the force of gravity. However, the system may adequately use non-overlapping voxels in the axial direction to assure channel connectivity in the axial direction. For example, FIG. **5** shows voxels touching in the azimuthal direction to give 100% coverage. Furthermore, FIG. **4** shows the different sizes of the near and far voxels in the axial direction. For 100% coverage in the axial direction, the near voxels must contact which causes the overlapping of the far voxels.

FIG. **12** illustrates an extreme example of overlapping voxels in the azimuthal direction, as illustrated by arrow **44**, and non-overlapping voxels in the axial direction, as indicated by arrow **82**. The azimuthal overlap assures detection

of an elongated channel **78** during each complete rotation. In this example, channel axial continuity is evaluated only once per pitch. The faster the logging speed, the greater the pitch. The azimuthal overlap is determined by the rotational speed of the rotating sonde head **60** and the pulse rate of the transmitting transducers **30, 46** and **48**

For non-overlapping voxels in the axial direction, voxels form a helical spiral. To avoid axial overlap, the pitch of the helix is selected to exceed the largest axial size of any voxel. The intersection voxel **50** in FIG. **5** is interrogated by transducers **46, 30** and **48** for each given azimuthal position of the head. The objective of having all transducers inspect every voxel is to identify the location and orientation of any reflective boundary which might occur in any voxel. To select which voxels contain reflective surfaces, it is necessary to compare the relative amplitudes observed with each of the multiple viewing position transducers. The voxel corresponding to the first arrival behind casing in the propagation direction identifies the location of a surface reflection. The incidence angle of the transducer with the strongest amplitude signal from the voxel identifies the refracted angle of a reflecting surface within an occlusion or channel within the cement. The refracted angle determines the orientation of the normal to the reflecting surface, thus providing the inventive system with information necessary to construct geometry of occlusions, channels, or defects in the cement-casing interface. Therefore, both timing and amplitude of signals are required to select the probable location and orientation of the occlusion surface.

Unlike intersection voxel **50**, near and far voxels **36** and **38** require head rotation to have all transducers inspect a given voxel. The collection of data and the construction of images must have consistent voxel configurations. For a valid probability, all transducers must follow the same helix. If the helix inspected by one transducer is significantly shifted axially from the helix inspected by another transducer, changes in the reflecting surface with axial position may invalidate the measurement.

The inventive system disclosed herein minimizes problems with identifying the location and orientation of surfaces behind casing. The inventive imaging system includes adaptive voxel configurations to meet the needs for each borehole. For any given wellbore, the voxel radial thickness is determined by time window resolution (typically a few wavelengths in cement) in evaluating an output signal of any given receiving transducer.

D. Forming Images

The final step of the inventive data processing algorithm is to create images of surfaces behind the highly reflective layer (casing **14**). Since transmission through a highly reflective layer, such as steel casing **14**, is weak, the reconstruction of information for reflectors behind casing is an enormous signal enhancement problem. Thus, the inventive system subdivides processing into several stages, as discussed above. Each transducer output is enhanced separately in the time domain and compressed as described above. Transducer responses are combined uphole to form images, as discussed below.

1. Mode Identification

Wave propagation in a solid medium involves different modes (waves propagating at different speeds). For example, acoustic energy generated by transmitting transducers will travel at different speeds, depending upon the material through which the acoustic energy travels. For example, propagation speeds will be different for drilling fluid, steel, and cement and for shear and compressional waves. Proper identification of modes is necessary to transform voxel information uniquely from the time domain to the space domain. The multiple viewing position technique helps to identify modes by using ray tracing to calculate different propagation velocities and azimuthal positions. FIG. **13** schematically illustrates the direction and progression of various acoustic rays which represent the centers of acoustic radiation patterns from transmitting transducers **46, 30** and **48** through the casing **14**. The move-out of a reflected signal in time as the transducer rotates azimuthally is a key factor in confirming mode arrivals. The inventive system is configured to process modal information in the imaging algorithm by determining mode speeds that make all transducer processed outputs consistent.

2. Transforming From Time to Space Domain For Individual Transducers

The inventive system incorporates an algorithm which converts the time domain data from the receiving transducers into a crude image in the space domain. This algorithm organizes ray path information for reconstruction by ordering data on transducer and casing position and on propagation velocity behind casing. As illustrated in FIG. **13**, transmitting transducers **46, 30** and **48** have different ray paths in a horizontal plane. For example, transmitting transducers **46, 30** and **48**, each include ray paths **84, 86** and **88** for interrogating a specific intersection voxel within cement **12** beyond casing **14**. Arrows, **96, 98** and **100** represent the propagation of centers of acoustic radiation to and from an occlusion or channel within the cement **12**. Arrows **90, 92** and **94** represent refracted propagation of centers of acoustic radiation paths through the steel casing **14** to and from a reflective occlusion within the cement.

In processing the received acoustic signals, time domain amplitude information is transformed to space domain using the wave velocity and the angular orientation of the ray path. The beamspread of the radiation pattern is included by calculating the ray paths for the edges of the radiation pattern. The algorithm treats increasing voxel transverse width with increasing propagation distance. The procedure uses a ray tube concept to spread amplitude information as a function of propagation distance.

3. Adaptive superposition of different transducer contributions

Multiple viewing position transducers **46, 30** and **48** contribute independent radial and azimuthal information about reflectors behind casing. The inventive system utilizes different weighting factors to combine their independent measurements to determine voxel locations that contain reflective surfaces. For example, the transmitting transducer **30** in FIG. **5** receives stronger signals than the offset transducers for reflector surfaces having normals parallel to the radius of casing **14**. The inventive system detects reflector surfaces with normals tilted relative to the casing radius by selecting the offset transducers (transducers **46** and **48**) with a refraction angle most nearly coinciding with a normal to a reflector surface.

F. Image Enhancing

As discussed above, dense azimuthal coverage is needed for smooth images. For example, the image disclosed in FIG. **7** has 36 azimuthal observations. The inventive system may also include an interpolation grid stored to memory in order to obtain high resolution images. The inventive system utilizes several of such data smoothing techniques, as discussed below.

1. Imaging Smoothing

Image smoothing may be done in two steps. First, reflection wave amplitudes are redistributed in space using ray tube or energy spreading. Here, the system subdivides the

tubes to obtain a smaller grid spacing, which effectively increases the number of voxels but the total energy distributed amongst all voxels remains the same. Second, the inventive system smoothes the amplitude using a moving rectangular-image filter.

2. Coherent Enhancement and Suppression

As discussed above, due to reverberations, various arrivals may mask signals from the reflector behind casing. Some reverberations have distinctive patterns. For example, transducer ring-down and casing fluid multiple reverberations could create false images in the map of the region behind casing. These reverberations may have arrival times dependent on azimuthal position. Simple subtraction of reverberations may be insufficient. If subtraction of reverberations is insufficient, coherency analysis on a group of azimuthal observations may be more effective. Using coherency analysis allows the enhancement of images from reflectors (e.g., occlusions or channels) behind casing **14** while suppressing reverberations.

## III. Dual Distance Transducers

As discussed above, the casing **14** and fluid **32** trap reverberations which can mask echoes from reflectors in the cement **12**. An alternative embodiment of the present invention relates to a configuration which places transducers at two distances from the casing. FIG. **14** illustrates in sectional view an example of a radiation pattern configuration for pulse-echo transducers **30** and **34** positioned at dual distances from a geometric center of sonde rotating head **60**. For pulse echo, each transducer is operated separately at a different time than the other and senses reflectors anywhere in its radiation pattern. Both transducers detect reflector within overlapping main lobes (region **99**) as indicated between the intersecting 50% amplitude contours **22**. Different travel times in the fluid **32** between transducer and casing give different interference time of the fluid reverberations.

More specifically, the transducer configuration approach of FIG. **14** selects the fluid path of transducer **34** to have travel time exceeding the travel time of the transducer **30**. The extra travel time is chose to be approximately equal to the casing reverberation time. The transducer **34**, therefore, has no fluid reverberation during the time interval which is obscured by a first fluid multiple of the first transducer. Likewise, the transducer **30** has minimal reverberation during a first fluid multiple of the second transducer. For each successive time window between fluid multiples, a processor selects the transducer with minimal reverberation. This configuration improves the ratio of third medium (cement **12**) reflector echo to reverberation noise.

FIG. **14** shows illustrates different fluid path lengths for transducers **30** and **34**. Transducer **30** has path length, d0. Transducer **34** has path length, d+d0. Transducers **30** and **34** are sufficiently axially separated so that one transducer does not insonify (impinge with acoustic energy) the face of the other and thereby receive fluid multiples from the face of the other transducer. In this configuration, transducer **34** must be elevated axially to inspect the same voxels as are inspected by transducer **30**. Logging apparatus **10** (shown in FIG. **1**) includes processing means in digital computer **2** to compensate for axial elevation differences between transducers by storing waveforms from the two transducers, recalling the waveforms and comparing them at identical elevations within wellbore **13**.

FIG. **15** illustrates the transducer configuration of FIG. **14**, schematically representing ray tracing of wave propagation for transducers with two different path lengths in fluid. FIG. **15** illustrates the wave propagation as rays instead of beams. The rays travel uninterrupted to the casing. More specifically, FIG. **15** shows a ray from transducer **30** enter casing **14** and reverberate to produce a first reflection or reverberations **62**. The rays complete a round trip and return to location A1 on Transducer **30**. Similarly, rays from transducer **34** enter casing **14** to produce a first reflection or reverberations **65** and return to location A2 on transducer **34**. Rays reflected at locations A1 and A2 by the faces of transducers **30** and **34** generate fluid multiples **64** and **67**, respectively. The first fluid multiples make second round trips in fluid **34** (as mentioned, the first round trips return to locations A1 and A2) and return to locations B1 and B2, respectively, for transducers **30** and **34**, respectively. The second fluid multiple makes a third round trip **66** in fluid and returns to C1 for transducer **30**.

FIG. **16** illustrates the signals obtained for the dual distance transducers **30** and **34** shown in FIG. **15**. The echoes at A1 and A2 arrive at times $\Delta t0$ and $\Delta t1$. The echoes at B1 and B2 arrive at $\Delta t0+\Delta t2+\Delta t3$ and $\Delta t1+\Delta t2+\Delta t3+\Delta t4$, respectively. An important feature to note is that the time between A1 and B1 is different than the time between A2 and B2. No fluid multiple occurs for transducer **34** during time window $\Delta t4$. This quiet time interval for signal **2** permits inspection of the cement located behind casing at a radial distance range from x1 to x2 where:

$$x1=v*(\Delta t2+\Delta t3) \quad (9)$$

$$x2=v*(\Delta t2+\Delta t3+\Delta t4); \text{ and} \quad (10)$$

v=acoustic energy propagation speed in cement.

Similarly, the radial distance range behind casing corresponding to $\Delta t5$ is inspected with transducer **30** via signal **1** because transducer **34** has its first fluid multiple during that time interval.

FIG. **17** illustrates an alternative embodiment of the transducer configuration having two transducers **122** and **124** embedded in the sonde head **60** at different azimuths in the radial plane. The configuration of FIG. **17** is significantly different than that of FIG. **14**, but achieves the same result. More specifically in this configuration, transducers **122** and **124** have separate azimuths instead of the separate axial locations shown in FIG. **14**. For separate azimuths, the same echoes through fluid **32** from casing **14** and cement **12** occur as illustrated by the waveforms in FIG. **16**, and the same calculations for arrival times apply as set for above, taking into account distances d and d0. The digital computer **2** in logging apparatus **10** includes processing hardware and software to compensate for azimuth differences between transducers, by comparing waveforms generated by transducer **122** to those generated by transducer **124**, by taking into account the azimuthally desperate locations of transducers **122** and **124**, in a manner similar to the process for the transducer configuration of FIG. **14**. More specifically, waveforms for identical azimuths can be compared for the two transducers by using stored data in the manner described above.

FIG. **18** schematically illustrates another embodiment of the inventive transducer configuration which includes vertical, radial and azimuthal separations between two pulse-echo transducersl22 and **124** embedded within sonde head **60**. By having offsets in the radial, azimuthal and axial directions as shown in FIG. **18**, the transducers can log nonoverlapping helical paths. If the logging axial speed and rotational speed are controlled to have an axial translation of distance, h, in the time that the head rotates 90°, then

transducers **122** and **124** will insonify exactly the same helical path. The inspection time for transducer **122** will occur later by a fourth of the rotational period. Another advantage of having two transducers is the capability to make a downhole measurement of the fluid speed of sound. The fluid paths of transducers **122** and **124** differ by distance d. Dividing d by the difference in travel times to the inner surface of the casing gives speed of sound of the fluid. This measurement is especially important in oil base drilling fluids having dissolved natural gas. Dissolved gas gives unexpectedly small fluid speeds of sound, which leads to inaccuracy in the calculation of distances in fluid.

FIGS. **19**(*a*) and **19**(*b*) illustrate a cylindrical test wellbore configuration including a central casing **14**, a cement annulus **12** surrounding and supporting the casing, several test channels **78** formed in the cement annulus, and an outer casing **52** (simulated hard formation). This laboratory version includes the essential features encountered downhole. The specimen shown in FIGS. **19**(*a*) and **19**(*b*) was inspected by placing a pair of transducers inside the inner casing. The echoes resembled those of FIG. **16**, except that the baseline signal included noise. For example, the baseline noise in time window, Δt3, had amplitude approximately one tenth that of the fluid multiples. The echo from reflector in cement was larger than the baseline noise but smaller than the amplitude of the multiples.

As discussed above, the dual distance transducer configuration embodiment utilizes different fluid multiple path distances to provide time windows that are free of fluid reverberations and therefore achieves a good signal to noise ratio for receiving signals from reflectors within cement **12** behind casing **14**. If one transducer has fluid reverberations obscuring parts of a first region behind casing, the second transducer has a time window without reverberations for that first region behind casing. If fluid reverberations obscure a second region for the second transducer, the first transducer can have a reverberation free time window for the second region.

FIGS. **20**(*a–c*) illustrate a sonde head having dual-distance transducers at a single azimuthal location. In this embodiment, rotating head **60** includes a tilted receiving transducer **136** disposed between two transmitting transducers **134** and **132**. Receiving transducer **136** is so narrow that no multiples are produced by reflections from its surface and that its main lobe receives radiation from both transmitting transducers **134** and **132**. The transmitting transducers **134** and **132** each have a main lobe width that is selected to include the receiving transducer **136**. Receiving transducer **136** lies within in the main lobe of the radiation pattern from each of transmitting transducers **132** and **134**, but the transmitting transducer **132** lies within the null between the main lobe and the first side lobe of transmitting transducer **134**, and likewise transmitting transducer **134** lies within the null between the main lobe and the first side lobe of transmitting transducer **132**. This configuration permits the voxels in cement **12** to be essentially coincident for both dual-distance firings through fluid **32** and casing **14**. The dual distance transducers may be used with other sets of transducers to form a more a complete image of the region behind casing. For example, the center transducer in FIG. **5** which is oriented in the normal direction relative to casing surface may incorporate the dual-distance transducer in FIGS. **20**(*a–c*). In that embodiment, the intersection voxel **50** has the same azimuth for all three transducers shown in FIG. **5**. As seen in FIGS. **20**(*a–c*), the voxel elevations for the two transmitters are almost identical also. The localized intersection voxels **50** permit transducers to be sequentially fired as a helical swath is inspected. Since the head does not have to rotate or elevate to have both transmitters fire in a given voxel, the insonified helix can have any desired axial pitch. However, voxels are usually selected to overlap in the azimuthal direction to assure channel detection, as discussed above. In the axial direction, voxels may be nonoverlapping to permit faster inspection rates, as is also discussed above. Characterizing axial channels that permit fluid communication behind casing requires azimuthal but not axial overlap of voxels. The axial locations are shown as helical but may have other patterns which give the desired coverage to effectively characterize the axial connectivity of channels.

FIG. **21** illustrates a block diagram of the algorithm of the processing sequence for imaging behind reflective layers with a dual-distance transducer configuration in accordance with the present invention. Applicants have found that processing waveforms of FIG. **16** from both transducers also gives good signal to noise for all regions behind casing. Referring to FIG. **21**, transducers **122** and **124** each send a pulse **126** and **128**, respectively, as illustrated in block **138**, producing the waveforms illustrated in FIG. **16**. Each transducer receives its first reflection, **62** and **65**, respectively, as indicated by block **140**, and the time for reflection is recorded, as indicated by block **142**. As indicated by block **144**, the signals may then be processed in several forms. The processing means within the sonde **16** or digital computer **2** may combine waveforms from both transducers. For example, if neither waveform has a fluid multiple in a time window, the average of both waveforms is used in that window. Alternatively, time windows of one waveform having a fluid multiple may be disregarded while the other waveform is used without averaging for that spatial region behind casing **14**. As discussed above, the timings of windows are calculated from the travel times to obtain the first reflection from the inner casing wall. Finally, the processing means in digital computer **2** or sonde **16** may further image process the processed waveforms to create the final image, as indicated by block **146**.

## IV. Multiple View Positioning

In an alternative embodiment of the present invention, the transducer configuration is arranged and configured to improve acoustic imaging of the region surrounding the rotating sonde head **60** (FIG. **1**) by utilizing multiple collimated transducers. In this embodiment, multiple beams cover a spread of propagation directions relative to the radial direction, illustrated by arrow **44** in FIG. **22**. As discussed above, in drilled wells, acoustic transducers are used to image the distance to a acoustically reflective surfaces, which represent occlusions or channels in concrete **12** surrounding casing **14**. The timing and amplitude of reflected signals are processed to map azimuthal and radial locations of the reflective surfaces relative to the direction of propagation.

If the reflector surface of an occlusion or channel is tilted relative to a normal the incident acoustic wave, reflected acoustic waves do not return to the receiving transducer, which causes the imaging method to fails. For example, FIG. **22** shows a configuration in which the propagating wave does not return to the rotating head **60**. There, an acoustic wave propagates from pulse-echo transducer **22**, reaches reflective surface **154**, at an angle of incidence ox with respect to surface normal **150** and returns at an angle of reflection β, which is approximately equal to angle α. The reflected wave misses the rotating sonde head **60** completely.

This embodiment of the present invention maps first reflector azimuthal and radial locations for a wide range of

reflecting surface angles. The inventive configuration and method applies to not only a first reflecting surface encountered, but also to subsequent reflecting surfaces. Therefore, the inventive configuration may map casing surface **12**, the casing-cement interface and the cement-earth formation interface using refracted waves media beyond the casing **14**.

This embodiment of the transducer configuration invention uses multiple transducers on a rotating head radially displaced from the center of rotation. For example, FIG. **23** shows three transducers **122**, **124** and **148** in rotating head **60** having radius R. Each transducer insonifies (sends acoustic energy through) a fixed range of angles relative to the radial direction. Transducer **148** detects surface **154** orientation at location Z, which was previously undetectable for the transducer configuration illustrated in FIG. **22**. Transducer **122** detects the surface **154** at location X, which was also undetectable for the transducer configuration illustrated in FIG. **22**. Transducer **124** detects a corner reflector in the surface **154** at location Y.

In the embodiment illustrated in FIG. **23**, transducer beams are designed to have sufficient beamspread cover to have a range of propagation directions. The selection of a slight overlap of beamspreads from adjacent transducers obtains complete coverage of inspection directions relative to the radial direction. As the rotating sonde head **60** rotates, transducers remain a fixed radial distance from the center of rotation. In one full rotation, the boundary at surface **154** can be mapped. Reflecting surfaces perpendicular to any transducer beam return echoes to the corresponding transducer. FIG. **24** illustrates that reflecting surface normal vectors must intersect the rotating head **60** to be imaged. Surface normal vectors v and w do not intersect the tool head of radius R. Therefore, a larger head radius is required to image Locations v and w.

If the sonde **16** is carefully centered in casing **14**, transducers **122**, **124** and **148** have fixed angles of incidence with respect to casing **14**. For example, in FIG. **25**, refracted angles in casing **14** and cement **12** are related to angle of incidence via Snell's Law. The refracted angle in cement **12** is affected little by casing **14** and mostly by properties of fluid **32** and cement **12**. With or without casing **14**, reflective surfaces in cement **12** can be imaged, provided that the rotating head **60** is centered within a circular borehole in fluid **32**. The ordinarily skilled artisan will also recognize this beamspread overlap configuration may be applied more generally to any set of imaging transducers provided that angles of incidence remain fixed as transducers are scanned along the surface between fluid **32** and cement **12**. In particular, if transducers **122**, **124** and **148** are in a pad that travels along the surface between fluid **32** and cement **12**, incidence angles can be carefully controlled. This pad configuration may have many applications including that of cement imaging in cased wells.

FIG. **26** shows the rotating sonde head **60** rotated slightly counterclockwise from the position in FIG. **23**. No reflected waves return to the transducer from which they were transmitted. However, the acoustic wave **160** from transducer **148**, however, does return to the transducer **122**. This pitch-catch operation of transducers **122** and **148** aids in imaging tilted reflective surfaces. For example, a location X, now similar to location v in FIG. **24**, the reflected acoustic wave **156** from transducer **122** does not does not return to transducer within the configuration. In this example larger rotating head **60** may be needed to detect location X.

FIG. **27** shows transducer **124** transmitting radially, having a beam **158** which strikes the reflecting surface **154** at normal incidence. When the borehole surface is circular and concentric with the rotating head **60**, radially-directed transducers can operate in either pulse-echo or pitch-catch modes. When operating in a pitch-catch mode, the nulling reverberation method described above with the vertical configuration of a transducer pair used may be utilized. Therefore, the top view in FIG. **27** applies to either pulse-echo or pitch-catch modes. FIG. **5** illustrates a top view for imaging behind casing in that matter, wherein nulling of casing reverberations enhances imaging signals associated with the cement **12**. FIGS. **2** and **4** show vertical views for pulse-echo and pitch-catch modes, respectively.

As described above, the inventive apparatus **10** must process data for each direction of insonification for each azimuthal orientation of the rotating head **50**. Images are constructed by dividing material surrounding the head into voxels as shown in FIG. **5** and recording reflective energy for each voxel, for each transducer. For each voxel, a summed weighting of signals from all transducers is used to obtain an estimated reflectivity and probable reflective surface orientation for the voxel.

By linking amplitude contours and surface orientation contours, the inventive system forms a map by connecting the contours from voxel to voxel. The first strong intensity change is called standoff. A map of standoff versus azimuthal orientation of the rotating head **60** gives a caliper of the first reflective boundary. If the first boundary is the borehole wall, the image provides borehole wall geometry and hence becomes a borehole caliper.

To image behind casing as in FIG. **25**, voxels can be mapped just for the region behind casing as shown in FIG. **5**. Several approaches can be used to improve imaging of reflectors behind casing. In FIGS. **25** and **5**, the central transducer radiates along the casing **14** diameter and receives strong echoes from casing inside diameter (ID), wall thickness and wall reverberation. To image a reflector (e.g. an occlusion or channel) within cement **12** behind casing **14**, the reflector normal must be collinear with the diameter of casing **14**. In this case, the above-described dual-distance transducer configuration offers an approach to reduce problems with multiple reverberations in casing fluid **32** that obscure echoes from reflectors within the cement **12** or the earth formation behind casing **14**.

The two outer transducers in FIGS. **25** and **5** have propagation directions at angles with the casing diameter. Incidence angles for waves entering casing affect not only casing reverberations but also refraction angles. As discussed above, incidence angles can be selected to strengthen refracted waves behind casing **14** while weakening casing reverberations reaching the receiving transducer. To inspect a range of angles behind casing, incidence angles of beams for Transducers **122** and **148** can be selected to overlap the beam of transducer **124** in an overlap voxel as shown in FIG. **5**. This overlap improves imaging for non-overlapping helical spiral inspection paths. The incidence angles are selected to obtain the desired range of refracted angles behind casing. As illustrated in FIG. **25**, refracted angles remain constant relative to the casing diameter as the head **60** rotates azimuthally. A reflective surface within the cement **12** behind casing **14** returns a signal when any transducer produces a wave propagating collinear to a reflective surface normal.

In general, the concept of designing transducers with multiple viewing position imaging as illustrated in FIG. **25** has application to situations amenable to a rotating head **60** for inspecting surroundings to identify and locate irregularly

shaped acoustic boundaries. Besides wells, sewers, pipelines and in vivo passages could be inspected from the interior. The ordinarily skilled artisan, however, will recognize that the rotating head **60** and cylindrical geometry of the sonde **16** are not essential to the transducer configuration concepts disclosed herein. The inventive apparatus and method applies to any configuration having voxels in a first medium (e.g., cement **12**) inspected from multiple angles using multiple transducers in a second medium (e.g., fluid **32**) that scan the boundary between the first and second media. The first medium (e.g., cement **12**) can be inspected using heads on either interior or exterior boundaries.

FIG. **28**(*a*) shows a specimen which includes casing fluid **32** (water), inner casing **14**, cement **12** and an outer casing **52** (simulated hard formation). The laboratory version of the transducer configuration included transducers in specimens containing the essential features encountered downhole. The specimen shown in FIG. **28**(*a*) was inspected by placing three pairs of transducers inside the inner casing. FIG. **4** shows a side view of one pair of transducers. FIG. **5** shows a top view of the three pairs of transducers. A fourth pair of transducers oriented the same as the central pair (FIGS. **5** and **4**) but at a different distance from the casing **14** to reduce reverberation problems in the fluid **32**, as described above in the dual distancing section. FIG. **28**(*b*) illustrates an image formed using the processing techniques disclosed herein. Darker images imply stronger reflections. The dark gray regions coinciding with a circle depicting the cement-to-outer casing boundary **162** demonstrate imaging of a reflecting surface eccentered from inner casing **14**. No existing commercial system can produce an image of this boundary.

As discussed above, the rotating sonde head includes apertures for exposing the transducer faces to the fluid **32** within the wellbore. Aperture modeling traces rays on collimated and divergent edges of transducer-radiation patterns. A method in accordance with the present invention simplifies analysis of size transducer faces to select beam patterns. The inventive method utilizes a model which estimates collimation and divergence of beams passing from transmitter through casing fluid **32**, casing **14** and cement **12** and returning to a receiving transducer. As discussed above, FIG. **2** schematically illustrates beamspread geometry in the axial (vertical) plane; and FIG. **5** shows central rays for three radial-plane-transducer pairs (radial-plane rays are top views of axial-plane rays in FIG. **2**). The central ray of the center transducer pair **30** illustrated in FIG. **5** propagates along a casing radius and enters cement **12** normal to the casing surface.

On the other hand, rays from the outer transducer pairs **44** and **46** in FIG. **5** are parallel to the ray associated with the center pair **30**, but offset. This offset corresponds to tilting pair faces as illustrated in FIG. **25**. The tilting pair faces comprise an incidence angle, $\theta_i$. One outer pair tilts clockwise and the other counterclockwise.

The beam pattern for the clockwise transducer in FIGS. **25** or **5** is shown in FIG. **29**. The central ray refracts at clockwise angle, $+\theta_{cc}$, relative to casing normal at the steel-to cement interface. At the beam edges, the beamspread angle, B, contributes to the angle of incidence. The resulting refraction angle at the left edge is $\theta_{cc}-B_{cc}$ and at the right, $\theta_{cc}+B_{cc}$. The edge and center rays from the counterclockwise pair mirror those of FIG. **29** which results mathematically by substituting $+\theta_{cc}=-\theta_{ccc}$; and $B_{cc}=-\theta_{ccc}$.

The center pair in FIG. **5** has central-ray-refracted angle, $\theta_{cn}=0$. Incidence angles of rays at half-amplitude edges of the beam depend on B and on casing curvature. In cement **12** beyond casing **14**, refracted beamspreads are $-B_{cn}$ at the left edge and $+B_{cn}$ at the right edge. FIG. **5** also illustrates the essence of multiple-viewing-position (MVP) imaging for the cement annulus. As discussed above, that configuration allows each voxel to be interrogated from multiple directions. Multiple steering angles require transducer-radiation patterns adequately collimated in cement to prevent interference from reflectors in adjacent voxels. Beamspread, controlled by transducer size and frequency, is optimized to detect all relevant-reflector angles with the fewest transducer pairs.

Transducer radiation patterns can be selected to obtain complete coverage of relevant reflector angles. For coverage with three transducer pairs, select beamspread, $B_{cn}$, of the center pair as

$$+B_{cn}=+\theta_{cc}-B_{cc} \text{ and } -B_{cn}=+\theta_{ccc}-B_{ccc} \tag{11}$$

where $+B_{cn}$, is clockwise spread and $-B_{cn}$, counterclockwise spread of the central pair.

In FIG. **29**, the left edge of the clockwise beam lies at an angle of $\theta_{cc}-B_{cc}$ from the casing normal. Angles closer to the normal are outside the beam of the clockwise pair. Equation 11 assures that the central pair interrogates angles from O° to $\theta_{cc}-B_{cc}$ relative to the casing normal. For the counter-clockwise pair, the angle from the right edge to the normal is $\theta_{ccc}-B_{ccc}$, and $-B_{cn}$ of the central pair covers this angular region. Several aperture design trade-offs must be considered to select $\theta_{cc}$, $B_{cc}$ and $B_{cn}$ for the radial plane.

Regarding the first trade-off, one objective includes configuring the $\theta_{cc}$ angle to cover all relevant reflector orientations. A large $\theta_{cc}$ angle requires large $B_{cc}$ and $B_{cn}$ angles to cover all reflector orientations. Large $B_{cc}$ and $B_{cn}$ angles give a large transverse extent for far voxels and hence poorer channel resolution. If channel resolution is a problem, more than three transducer pairs will be needed to adjust $B_{cc}$ and $B_{cn}$. The first trade-off, therefore, optimizes the dual conditions: (1) a small number of transducers for higher tool reliability and lower cost tool; and (2) a small voxel size for good resolution of channels.

With regard to a second trade-off, a second goal is achieving fast logging speeds. Logging speed depends on the rotation speed of the sonde head **60**, transducer firing rate and helical coverage. As the transducer head **60** rotates, radiation patterns also rotate relative to the stationary casing **14**. As best illustrated in FIG. **5**, as the head **60** rotates, each voxel is interrogated by all three beams. For nonintersecting voxels, each beam interrogates the voxel at a different rotational position of the head. For example, in FIG. **5** transducer **48** investigates far voxel **40**. As the head **60** rotates in a further clockwise direction, transducers **46** and **30** also investigate far voxel **40**.

For large helical pitches, the voxel axial length illustrated in FIG. **4** controls axial coverage per rotation. Valid coverage requires interrogating each voxel from each viewing angle at a single axial depth in the well. In FIG. **5**, far voxels **42** and **40** are separated by intervening far voxel **38**. The center and clockwise transducer pairs **30** and **44** must rotate to interrogate far voxel **40** utilizing rays cc and n, respectively. Far voxel **40** will be interrogated in three different firing sequences. For large helical pitches during fast logging speeds, the transducer pair **44** could translate axially during this rotation. The resultant non-overlapping axial coverage could invalidate the criteria for inspecting each voxel from all relevant angles in the radial plane, however, the inventive system accounts for differing axial heights of each successive interrogation, as described above my recording axial position for each far voxel measurement. On

the other hand, during a single firing sequence, all three beams rapidly interrogate the intersection voxel **50** with very little rotation between firings. For the intersection voxel **50**, therefore, logging speeds can be faster than for widely separated far voxels.

The second trade-off involves minimizing the separation between far voxels. Referring back to FIGS. **29**, for large $\theta_{cc}$ angles, however, this best condition for far voxels has the disadvantage of maximizing the separation for near voxels. The second trade-off optimizes a trio of conditions: (1) small separations for far voxels; (2) small separations for near voxels; and (3) a large $\theta_{cc}$ angle. The resultant transducer configuration will insonify a helical swath of voxels when rotating and while translating axially in the borehole. The axial length of the swath will be the axial length of the voxel of interest, as illustrated in FIG. **4**. Although radial overlapping is required to achieve 10° resolution of channels, axial overlapping is unnecessary for interpreting channel connectivity. A swath once every 3 inches of axial travel is acceptable according to marketing surveys completed by Applicants, which show that as few as three measurements per radial plane give valid calipering (to determine cement thickness for formation evaluation).

The third trade-off involves beamspread angle, B, in FIG. **29** (or β in FIG. **2**). B depends on $V_i$, w, f, and frequency bandwidth Δf. Minimum B depends on:

$$w/\lambda = w*f/V_i \quad (12)$$

Bandwidth, Δf, and multimode speeds of sound, $V_i$, give rainbow-like spectral broadening of angle B. Narrow bandwidths improve beam-edge definition and hence voxel-transverse edges. As a penalty, narrow bandwidths give poor resolution in the propagation direction because wave packet time duration increases. Frequency-dependent attenuations in drilling fluid and cement also broaden B. Large f gives small B, giving better control of voxel size, but reduces signal strength due to attenuation. Fitting all transducers into the 3⅜" outside diameter of rotating head **60** constrains w.

The third trade-off, therefore, optimizes the six considerations: (1) high frequencies for small voxels; (2) low frequencies for penetration through drilling fluid and cement; (3) small bandwidths for good voxel resolution in the transverse direction; (4) large bandwidths for good voxel resolution in the propagation direction; (5) wide transducer elements for good voxel transverse resolution; and (6) narrow transducer elements to permit a small outside diameter for rotating head **60** for a small inside diameter of casing **14**. As discussed above, data processing algorithms include wavelet modeling to derive optimum frequencies, bandwidths and transducer widths for voxel resolution.

Another important aspect of the present invention involves selecting transducer radiation pattern angles. More specifically, an important finding is the need for a range of refraction angles to obtain cement-to-formation reflections for an eccentered casing. FIGS. **30** and **31** illustrate rotating head **60** in a clockwise direction, as shown by arrow **44**, within a cement-formation boundary **130**, to show that two transducer pairs are needed to interrogate opposite halves of the formation wall for an eccentered casing (not shown). For example, in FIG. **30**, rays **160** and **158** for transducer pairs **148** and **124**, respectively do not return to rotating head **60** after reflection from the cement boundary **130**, whereas only ray **156** returns to its originating transducer pair **122**. Similarly, in FIG. **31**, when rotating head is offset almost 180° from the position of FIG. **30**, ray **160** from transducer pair **148** returns to transducer pair **148** whereas rays **156** and **158** do to reach their originating transducer pairs **122** and **124** after reflection from cement-formation boundary **130**. Thus for each azimuthal position of rotating head **60**, at least one transducer pair must include in its radiation pattern a normal to an occlusion or channel within the cement **12**.

FIGS. **32**(*a*) and **32**(*b*) show that each multiple-viewing-position beam detects a cylindrical channel, but that beams interrogate cylinders from different refraction angles in cement. Specifically, in FIG. **32**(*a*), note that casing **14** refracts and focuses rays from transducer pairs **122**, **124**, and **148** on an intersection voxel as the sonde head rotates in the direction indicated by arrow **44** toward channel **78**. As the transducer configuration rotates toward the occlusion **78**, note that casing **14** focuses each of rays **156**, **158** and **160** from transducers **122**, **124** and **148** on an outer periphery of channel **78** in a near voxel.

FIG. **33** shows that when the intersection voxel is not at the center of the channel **78**, transducers **122**, **124** and **148** do not receive reflections simultaneously from channel **78**, and obtain a reflection from a cylinder at a different head azimuth. For example, in the azimuthal position illustrated in FIG. **33**, rays **156** and **160** deflect from channel **78**. Thus, only rays which travel coincident with a center of the channel **78** reflect back to the originating transducer pair, as is illustrated by ray **158**.

For typical casing sizes, the technique uses transducers of similar frequency (400 kHz), bandwidth (400 kHz), size (1.0 in.×0.4 in.) to those used in pulse-echo cement bond tools. Such transducers are built to withstand downhole temperatures of at least 350° F. and pressures at least 20,000 psi. The transducers are mounted on a rotating head similar to that of a conventional pulse-echo tool. The head requires accurate mounting angles and centralization in the bore of the casing to assure that the radiation patterns propagate in the required directions with the required standoff from casing.

The tool for the new technique requires sufficient slip-ring connections from each transducer element to the electronics in the stationary part of the tool. The system also includes sufficient downhole processing capability to perform signal enhancement and data compression, as discussed above. Additionally, the inventive system utilizes a telemetry data rate of approximately 180,000 bits per second to transmit information to the surface. The system also includes means for measuring transducer azimuth and elevation to create images as a function of depth in the well. Direction sensors in the tool-record orientation of the head. Logging sensors at the surface record elevation in the well. The amount of overlap between adjacent voxels is determined by the sampling rate and rotational speed of the head.

As schematically illustrated in FIG. **1**, digital computer **2** provides surface processing which is capable of reconstructing the compressed data transmitted along wireline **8**. Additionally, the inventive system includes conventional image displays **4** for forming images of the region behind cement from algorithms which perform the required processing from compressed data to acceptable images.

The inventive system is unique in that no existing commercial tools can image channels anywhere in the cement annulus **12** and caliper the radial thickness of the cement **12** as a function of azimuth and axial location. No existing instrumentation utilizes the concepts of enhancing data downhole to suppress reverberations, compressing data downhole for transmission and reconstructing data uphole to form images of reflectors behind a strongly reflective boundary. This inventive system can be of use in a variety of applications. Some examples include but are not limited to imaging cement in a dam using transducers in the water behind the dam, imaging organs in vivo through highly

reflective tissue, imaging the contents of sunken ships and determining the location of water passages behind highly reflective structures such as swimming pool walls, etc.

The foregoing has been illustrative of the features and principles of the present invention. Various changes or modifications to the invention may be apparent to those skilled in the art without departure from the spirit and scope of the invention. All such changes or modifications are intended to be included herein and within the scope of the invention.

What is claimed is:

1. A transducer configuration for use in acoustically imaging a target region behind an acoustically reflective layer, the transducer configuration comprising:

an in-the-oil-patch sonde having a rotating head constructed and arranged to support a plurality of transducers, the rotating head having a geometrical center;

a first transducer disposed within the rotating head at a first distance from the geometrical center, the first transducer for generating a first acoustic pulse and for receiving a first acoustic signal comprising a first reflection from the acoustically reflective layer, a first set of fluid multiples arising from reflections between the acoustically reflective layer and a surface of the first transducer, and a first signal associated with the target region; and

a second transducer disposed within the rotating head at a second distance from the geometrical center, the first distance being at least one wavelength different than the second distance, the second transducer for generating a second acoustic pulse and for receiving a second acoustic signal comprising a second reflection from the acoustically reflective layer, a second set of fluid multiples arising from reflections between the acoustically reflective layer and a surface of the second transducer, and a second signal associated with the target region; and

an adaptive multiplier mechanism configured to receive and process signals received by the first transducer and the second transducer at time intervals which occur between receipt of the first and second sets of fluid multiples, respectively, the adaptive multiplier mechanism configured to create a canceling signal having amplitude valleys therein such that the canceling signal promotes cancellation of the first and second sets of fluid multiples from the first and second acoustic signals, respectively.

2. The transducer configuration of claim 1 further comprising:

a mechanism for calculating an arrival time at the first transducer and the second transducer of fluid multiples based on acoustic wave travel time defined by a time interval between an acoustic pulse made by a transducer and receipt by that same transducer of the acoustic pulse reflection from the acoustically reflective layer.

3. The transducer configuration of claim 1 further comprising:

a mechanism for averaging signals generated by the first transducer and the second transducer during time intervals between receipt of fluid multiples, when the time intervals for the first and second transducers occur simultaneously.

4. The transducer configuration of claim 1 further comprising:

a mechanism for processing a signal generated by only one of the first transducer and the second transducer at time intervals when the other of the first transducer and the second transducer receives fluid multiples.

5. The transducer configuration of claim 1 wherein the first transducer and the second transducer are disposed in a vertically tandem relationship.

6. The transducer configuration of claim 1 wherein the first transducer and the second transducer are circumferentially distributed about the geometrical center of the rotating head.

7. The transducer configuration of claim 1 further comprising:

a transducer pair comprising the first transducer and the second transducer;

the rotating head including three transducers pairs disposed in a circumferentially adjacent relationship, wherein each transducer pair senses the same location with the target region for a given azimuthal position.

8. The transducer configuration of claim 7 wherein:

the first transducer pair and the third transducer pair comprise pitch-catch transducer pairs; and

the second transducer pair comprises a pulse-echo transducer pair, wherein the second transducer pair is disposed between the first transducer pair and the third transducer pair with respect to a circumference of the rotating head.

9. A transducer configuration for use in acoustically imaging a target region behind an acoustically reflective layer, the transducer configuration comprising:

a rotating head constructed and arranged to support a plurality of transducers, the rotating head having a geometrical center;

a first transmitting transducer disposed within the rotating head at a first distance from the geometrical center, the first transmitting transducer including a beamspread radiation pattern comprising a main lobe diverging from the first transmitting transducer, a side lobe disposed laterally adjacent to the main lobe, and a null region disposed between the main lobe and the side lobe, wherein the first transmitting transducer is adapted to generate a first acoustic pulse; and

a second transmitting transducer disposed within the rotating head at a second distance from the geometrical center, the first distance being at least one wavelength greater than the second distance, the second transmitting transducer including a beamspread radiation pattern comprising a main lobe diverging from the second transmitting transducer, a side lobe disposed laterally adjacent to the main lobe, and a null region disposed between the main lobe and the side lobe, the second transmitting transducer adapted to generate a second acoustic pulse;

a receiving transducer vertically disposed beneath the first transmitting transducer and above the second transmitting transducer;

a receiving surface on the receiving transducer disposed at a nonparallel orientation with respect to a vertical plane for detecting echoes from the first transmitting transducer and the second transmitting transducer, wherein the receiving surface includes a receiving beamspread radiation pattern having a main lobe diverging therefrom constructed and arranged to detect echoes from

the first transmitting transducer and the second transmitting transducer, and wherein the receiving surface dissipates acoustic reflections therefrom, thereby precluding receipt on the receiving surface of acoustic echoes associated therewith.

10. The transducer configuration of claim 9 wherein the main lobe of each transmitting transducer encompasses the main lobe of the receiving transducer, and wherein each transmitting transducer lies within the null region disposed between the main lobe and the first side lobe of the other transmitting transducer.

11. The transducer configuration of claim 9 further comprising:

a transducer set including the first transmitting transducer the second transmitting transducer and the receiving transducer;

the rotating head including three transducer sets disposed in a circumferentially adjacent relationship, wherein each transducer set senses the same location within the target region for a given azimuthal position.

12. In a transducer configuration for use in acoustically imaging a target region behind an acoustically reflective layer, wherein the transducer configuration includes a rotating head having a geometrical center and is constructed and arranged to support a plurality of transducers, a method comprising the steps of:

placing a first transducer within the roating head at a first distance from the geometrical center;

generating a first acoustic pulse with the first transducer;

receiving a first acoustic signal with the first transducer comprising a first reflection from the acoustically reflective layer, a first set of fluid multiples arising from reflections between the acoustically reflective layer and a surface of the first transducer, and a first signal associated with the target region;

placing a second transducer disposed within the rotating head at a second distance from the geometrical center the first distance being at least one wavelength greater than the second distance;

generating a second acoustic pulse with the second transducer;

receiving a second acoustic signal with the second transducer comprising a second reflection from the acoustically reflective layer, a second set of fluid multiples arising from reflections between the acoustically reflective layer and a surface of the second transducer, and a second signal associated with the target region;

creating a canceling signal having amplitude valleys therein such that the canceling signal promotes cancellation of the first set of fluid multiples and the second set of fluid multiples from the first acoustic signal and the second acoustic signal respectively; and

processing signals received by the first transducer and the second transducer at time intervals which occur between receipt of the first set of fluid multiples and the second set of fluid multiples, respectively, wherein signal values at time intervals between receipt of the first set of fluid multiples and the second set of fluid multiples provide acoustic waveforms associated with the target region.

13. The method of claim 12 further comprising the further step of:

calculating an arrival time at the first transducer and the second transducer of fluid multiples based on acoustic wave travel time defined by a time interval between an acoustic pulse made by a transducer and receipt by that same transducer of the acoustic pulse reflection from the reflective layer.

14. The method of claim 12 comprising the further step of:

averaging signals generated by the first transducer and the second transducer during time intervals between receipt of fluid multiples, when the time intervals for the first transducer and the second transducer occur simultaneously.

15. The method of claim 12 comprising the further step of:

processing a signal generated by only one of the first transducer and the second transducer at time intervals when the other of the first transducer and the second transducer receives fluid multiples.

16. The method of claim 12 comprising the further step of:

placing the first transducer and the second transducer in a vertically tandem relationship.

17. The method of claim 12 comprising the further step of:

circumferentially distributing the first transducer and the second transducer about the geometrical center of the rotating head.

18. The method of claim 12 comprising the further steps of:

creating transducer sets, each including the first transducer and the second transducer;

disposing three transducer sets in a circumferentially adjacent relationship on the rotating head; and

sensing the same location within the target region for a given azimuthal position.

19. In a transducer configuration for use in acoustically imaging a target region behind an acoustically reflective layer, wherein the transducer configuration includes a rotating head having a geometrical center, the rotating head constructed and arranged to support a plurality of transducers, the method comprising the steps of:

placing a first transmitting transducer disposed within the rotating head at a first distance from the geometrical center;

generating a first beamspread radiation pattern with the first transmitting transducer comprising a main lobe diverging from the first transmitting transducer, a side lobe disposed laterally adjacent to the main lobe, and a null region disposed between the main lobe and the side lobe;

generating a first acoustic pulse with the first transmitting transducer;

placing a second transmitting transducer within the rotating head at a second distance from the geometrical center, the first distance being at least one wavelength different than the second distance;

generating a second beamspread radiation pattern comprising a main lobe diverging from the second transmitting transducer, a side lobe disposed laterally adjacent to the main lobe, and a null region disposed between the main lobe and the side lobe, the second transmitting transducer adapted to generate a second acoustic pulse;

vertically disposing a receiving transducer beneath the first transmitting transducer and above the second transmitting transducer;

orientating a receiving surface of the receiving transducer at a nonparallel orientation with respect to a vertical

plane for detecting echoes from the first transmitting transducer and the second transmitting transducers;

generating a receiving beamspread radiation pattern having a main lobe diverging from the receiving surface;

detecting with the receiving beamspread radiation pattern echoes from the first transmitting transducer and the second transmitting transducer; and

dissipating acoustic reflections from the receiving surface, thereby precluding receipt on the receiving surface of acoustic echoes associated therewith.

**20**. The method of claim **19** comprising the further steps of:

encompassing the main lobe of the receiving transducer with each transmitting transducer; and

positioning each transmitting transducer within the null region between the main lobe and the first side lobe of the other transmitting transducer.

**21**. The method of claim **19** comprising the further steps of:

creating a transducer set including the first transmitting transducer, the second transmitting transducer and the receiving transducer;

disposing three transducer sets in a circumferentially adjacent relationship on the rotational head; and

utilizing all three transducer sets to sense the target region at the same location for a given azimuthal position.

* * * * *